



Citation for published version:

Tan, L, Reeksting, B, Ferrandiz-Mas, V, Heath, A, Gebhard, S & Paine, K 2020, 'Effect of carbonation on bacteria-based self-healing of cementitious composites', *Construction and Building Materials*, vol. 257, 119501. <https://doi.org/10.1016/j.conbuildmat.2020.119501>

DOI:

[10.1016/j.conbuildmat.2020.119501](https://doi.org/10.1016/j.conbuildmat.2020.119501)

Publication date:

2020

Document Version

Peer reviewed version

[Link to publication](#)

Publisher Rights

CC BY-NC-ND

University of Bath

Alternative formats

If you require this document in an alternative format, please contact:
openaccess@bath.ac.uk

General rights

Copyright and moral rights for the publications made accessible in the public portal are retained by the authors and/or other copyright owners and it is a condition of accessing publications that users recognise and abide by the legal requirements associated with these rights.

Take down policy

If you believe that this document breaches copyright please contact us providing details, and we will remove access to the work immediately and investigate your claim.

1 **Effect of carbonation on bacteria-based self-healing of**
2 **cementitious composites**

3
4 Linzhen Tan^a, Bianca Reeksting^b, Veronica Ferrandiz-Mas^a, Andrew Heath^a,
5 Susanne Gebhard^b and Kevin Paine^a

6
7 ^aBRE Centre for Innovative Construction Materials, University of Bath, UK

8 ^bDepartment of Biology and Biochemistry, Milner Centre for Evolution, University of Bath,
9 UK

10
11 **Corresponding author:**

12 Kevin Paine

13 BRE Centre for Innovative Construction Materials

14 University of Bath, UK

15 BA2 7AY

16 k.paine@bath.ac.uk

17

18 **ABSTRACT**

19 Self-healing cementitious composites are being developed to respond to the high cost of
20 repair and maintenance of infrastructure. A promising solution is the use of bacteria to
21 induce calcium carbonate precipitation within cracks when they occur and prevent further
22 deterioration. Previous work has shown successful bacteria-mediated self-healing of
23 cementitious composites at early-ages, in conditions where the material was uncarbonated
24 prior to cracking. However, as cementitious composites often crack when they have reached
25 a more aged state and are likely carbonated at the time of crack formation, these previous
26 experiments did not fully reflect the real-world situation. In the present study, we show that
27 for cementitious composites that do not carbonate prior to cracking the calcium hydroxide
28 created as a hydration product is a sufficient source of Ca^{2+} ions to provide effective
29 bacteria-induced healing. We note that supplying an extra source of Ca^{2+} ions at the moment
30 of cracking, delivered via encapsulation, further enhances the degree of healing. Importantly
31 however, in carbonated mortars calcium hydroxide is not available as a source of Ca^{2+} ions.
32 Consequently, we show for the first time that bacteria-based self-healing in mortars that
33 have carbonated prior to cracking is almost totally dependent on the availability of Ca^{2+} ions
34 released from an encapsulated source. Our study therefore provides important insights for
35 the rational design of self-healing concrete, where the conditions of the concrete during
36 service life need to be taken into consideration when choosing between direct addition or
37 encapsulation of calcium sources to ensure optimal performance.

38

39 **Keywords:** cracking; carbonation; self-healing; bacteria; concrete; mortar

40 1. INTRODUCTION

41 Concrete dominates our built infrastructure due to its reliable strength, durability, versatility
42 and thermal mass. However, concrete is relatively weak in tension and invariably cracks in
43 service. These cracks can act as pathways for the ingress of deleterious substances, which
44 may impair structural performance by instigating chemical attack on the reinforcing steel or
45 the cementitious matrix itself. It has been calculated that within the UK the annual cost of
46 repairing our infrastructure (mainly concrete) is £40bn, and the cost of disruption may be an
47 order of magnitude higher again [1]. As an alternative to repair, there has been much interest
48 in developing concretes and other cementitious composites that are able to self-heal their own
49 cracks and consequently reduce or even eliminate maintenance costs.

50 A number of techniques to provide self-healing in cementitious composites have been
51 described in recent years, including stimulated autogenous methods (for example,
52 superabsorbent polymers [2] and crystalline admixtures [3] that accelerate the formation of
53 cementitious hydration products on the surfaces of the crack), and autonomic approaches
54 (using minerals or polymers in an encapsulated form [4,5] or via vascular networks [6]) that
55 release materials that hydrate or harden to fill the crack. These and other approaches have
56 been described in detailed state-of-the-art reports [1,7].

57 A further autonomic approach is to utilise microbiologically induced calcite precipitates as a
58 healing product. This can be achieved by embedding spores of appropriate bacteria within
59 the concrete alongside nutrients to promote their growth. When a crack forms and water and
60 oxygen ingress, the spores germinate into active cells. In an environment rich in dissolved
61 inorganic carbon (DIC) and Ca^{2+} ions the bacteria aid and accelerate the precipitation of
62 calcium carbonate, usually as calcite, within cracks [8–11]. There are a number of pathways
63 by which bacteria may precipitate calcium carbonate [12,13], but they all generally require:
64 (i) a sufficient concentration of DIC within the pore water within the vicinity of the crack to
65 enable formation of CO_3^{2-} ions, (ii) a change in local pH; (iii) attraction of Ca^{2+} ions to the

66 negatively charged surface of the bacteria, where the bacteria may act as a nucleation point;
67 and (iv) a sufficient quantity of Ca^{2+} to precipitate calcium carbonate.

68 The ability of bacteria to autonomously heal cracks in cementitious composites by
69 precipitating calcium carbonate has been verified in several studies using a number of
70 technologies [14–21]. Since both Ca^{2+} and CO_3^{2-} ions are required, technologies have been
71 developed that provide these as separate additions (e.g. urea plus calcium nitrate), or by the
72 use of organic calcium salts (e.g. calcium lactate) which supplies both in a single additive.
73 Although the precise source of Ca^{2+} ions used by the bacteria during self-healing is unclear,
74 it has been proposed that calcium hydroxide is likely to be the most important source [22].
75 Therefore, it is interesting to note that in all previous studies, self-healing of the cracks has
76 been tested on water-cured mortars or concretes at a relatively young age (~28 days) where
77 calcium hydroxide is present as a hydration product and provides a plentiful supply of
78 soluble Ca^{2+} ions. Thus, it has been questioned to what extent the addition of further Ca^{2+}
79 ions is necessary [23].

80 That said, in many real-life environments, particularly those where the concrete is subject to
81 alternate wetting and drying, a process of carbonation can occur before the concrete cracks.
82 Here, environmental CO_2 dissolved in pore water accesses the concrete and, through a
83 series of reactions, calcium hydroxide is converted to calcium carbonate. The outcome is
84 that Ca^{2+} ions become trapped in a less soluble form [24]. Since there is no evidence that
85 bacteria can utilise the Ca^{2+} ions in calcium carbonate, there is a concern that bacteria-
86 based self-healing may not occur in concrete that has carbonated before cracking.

87 Furthermore, the quantity of CO_3^{2-} ions available for self-healing is related to the
88 concentration of DIC in the vicinity of the crack when it occurs. Whilst this may be
89 supplemented by the use of urea ($\text{CO}_2(\text{NH}_2)_2$) or organic salts, it should be noted that yeast
90 extract is nearly always used as an addition to bacteria-based cementitious composites to
91 promote germination of the spores and growth of the cells. Yeast extract contains carbon,

92 and it is likely that its metabolic breakdown provides a sufficient source of DIC. However, this
93 has not yet been proven.

94 The research described in this paper was carried out to ascertain for the first time whether:

95 1. Self-healing occurs in mortar that has carbonated prior to cracking; when: (i) the
96 calcium source is added directly to the concrete mix and (ii) when the calcium source
97 is encapsulated.

98 2. Yeast extract could be used as the sole added source of DIC, thus eliminating the
99 need for urea and organic salts and consequently simplifying mix designs.

100 For reasons of scale, the work carried out in this paper, as in other leading studies on self-
101 healing cementitious composites [9,21,25], has been performed on mortars where the
102 maximum aggregate size is ~4 mm. However, given that the cracks in concrete generally
103 form and propagate in the mortar phase, the results of this work are equally applicable to
104 self-healing of concrete and other cementitious composites.

105 **2. MATERIALS AND METHODS**

106 **2.1 Bacterial Strain**

107 The alkaliphilic species *Bacillus cohnii* DSM 6307 was obtained from the German Collection
108 of Microorganisms and Cell Culture (DSMZ), Braunschweig, Germany. They were stored in
109 50% (v/v) glycerol at -80 °C. To routinely culture *B. cohnii*, lysogeny broth (LB) was mixed
110 with alkaline solution (10% v/v) which contained 100 ml/l Na-sesquicarbonate (42 g/l
111 NaHCO₃ and 53 g/l Na₂CO₃ anhydrous) to adjust to pH 9.5.

112 Bacterial spores were grown in sporulation medium and harvested after 48 hours by
113 centrifugation [26]. Spores were collected by centrifugation at 3800 x g for 10 minutes, and
114 the spore pellet was washed thrice with chilled 10 mmol/l Tris-HCl buffer pH 9.

115 Chlorohexidine digluconate (0.3 mg/ml) was applied afterwards to kill vegetative cells
116 followed by a further three washes with the same Tris-HCl buffer. Spore pellets were snap-
117 frozen in liquid nitrogen and freeze-dried under vacuum overnight. Viability of spores (colony
118 forming units (cfu) per gram dry weight) was determined by dilution plating.

119

120 **2.2 Growth Media**

121 The growth media (GM) used in this study was comprised of calcium nitrate and yeast
122 extract. Both calcium nitrate and yeast extract were supplied by Sigma-Aldrich Corporation.
123 The GM were either adding directly into mortar matrix or encapsulated in lightweight aerated
124 concrete granules (ACG).

125

126 **2.3 Aerated concrete granules**

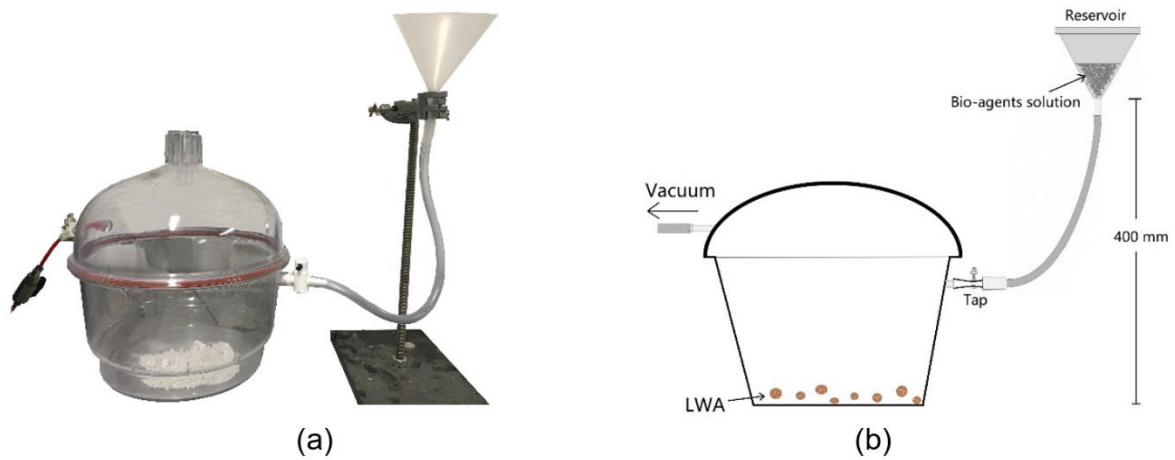
127 The ACG used were a commercially available product supplied by Cellumat SA Belgium.
128 They were used as the porous media for immobilisation of the spores, and as a carrier for
129 calcium nitrate and yeast extract in selected mixes. The ACG, as supplied, were separated
130 to produce a particle size distribution conforming to a 0/4 mm aggregate as defined in BS EN
131 12620. The ACG, as used, had a water absorption capacity of 120% and a loose dry bulk
132 density of 354 kg/m³.

133

134 **2.4 Encapsulation Process**

135 Both the bacterial spores and GM were encapsulated in ACG under vacuum. The
136 procedures were done independently to create ACG containing spores and ACG containing
137 GM. The method for vacuum impregnation was based on that described by Alghamri *et al*
138 [27]. A vacuum chamber with two-entry valves was set up as shown in Figure 1. One valve
139 was connected to a reservoir containing a suspension of spores or a solution of GM, whilst
140 the second valve was connected to the vacuum channel at 0.8 bar. For ACG containing
141 spores, a batch was made by resuspending spores (12.5×10^{10} cfu) in 10 ml distilled water
142 which was then imbibed into 18 g ACG. For ACG containing GM, the GM (4.55 g calcium
143 nitrate and 1 g (or 4g) of yeast extract) was dissolved in distilled water before being imbibed
144 into the ACG. The amount of distilled water within the suspension or solution equalled the

145 total water absorption capacity of ACG ensuring that the ACG were entirely saturated after
146 encapsulation.



147
148 *Figure 1 Vacuum encapsulation set-up, (a) on site, (b) schematic*

149
150 After the encapsulation process, the ACG were placed in an environmental chamber at 50%
151 relative humidity and 20°C for 24 hours to obtain a dry surface. Following this the ACG were
152 coated with PVA (polyvinyl acetate), supplied by BOSTIK Ltd, to provide a waterproof
153 protective layer. To achieve an even distribution of coating on the ACG, a Kenwood Major
154 Titanium Mixer with a K-Blade was utilized. Mixing proceeded until PVA was slightly dried on
155 the surface of ACG in case of any adhesive between particles. Thereafter, the coated ACG
156 containing spores (ACGS) and coated granules containing GM (ACGM) were stored in air-
157 tight plastic bags until used in mortar mixes.

158 The mass of the coating for ACGS and ACGM was approximately 33% of the overall mass
159 of the coated ACG and consequently the number of spores was approximately 6.9×10^9
160 spores per g of coated ACG. Less than 6% of coated particles by mass passed a 2 mm
161 sieve, compared with approximately 35% by mass passing this sieve prior to coating.

162

163 **2.5 Preparation of mortar specimens**

164 A series of mortars were produced using Portland limestone cement (CEM II/A-L 32.5R),
 165 standard sand conforming to BS EN 196-1, tap water and (i) ACGS and ACGM, or (ii) GM
 166 directly added to the mortar matrix (without encapsulation). The mix proportions are given in
 167 Table 1. The reference mortar (REF) was a standard cement mortar mix with water to
 168 cement ratio of 0.5 conforming to BS EN 196-1. A control mortar (CTRL) was made to
 169 assess the effect of the direct addition of growth media (4.55g calcium nitrate and 1g yeast
 170 extract) on the performance but without the addition of any spores.
 171 The final three mortars (CaN-direct, CaN-encap and CaNY-encap) all contained spores in
 172 the form of the addition of 5.25 g of ACGS – approximating to 3.64×10^{10} spores. For CaN-
 173 direct mix, the growth media were added directly to the mortar as per CTRL. For CaN-encap,
 174 the growth media was added in the form of 22 g of ACGM (which equalled the addition of
 175 4.55 g calcium nitrate and 1 g yeast extract). For the final mortar, CaNY-encap, the ACGM
 176 contained 4.55 g of calcium nitrate and 4 g of yeast extract, i.e. it had a higher quantity of
 177 yeast extract.

178

179 Table 1 Mix proportions for all mortar samples

Specimens	Cement (g)	Water (g)	Standard sand(g)	Yeast extract(g)	Calcium nitrate(g)	ACGS (g)	ACGM (g)
REF	92	46	276	0	0	0	0
CTRL	92	46	276	1	4.55	0	0
CaN-direct	92	46	260	1	4.55	5.25	0
CaN-encap	92	46	207	0	0	5.25	22.0 (contains 4.55 g calcium nitrate, 1 g yeast extract)
CaNY-encap	92	46	207	0	0	5.25	25.0 (contains 4.55 g calcium nitrate, 4 g yeast extract)

180

181 Mixing was carried out in accordance with BS EN 196-1 with the ACGS and ACGM added at
 182 the same time as the sand. Mortars were cast into prisms of dimension 65 mm × 40 mm ×
 183 40 mm. Specimens were comprised of two layers. To conserve spores, only the lower layer
 184 (20 mm deep) was self-healing mortar (as per the proportions in Table 1), whilst the upper
 185 layer (20 mm) contained REF mortar. The lower layer was cast first. After approximately 60

186 minutes the upper layer was then cast on top. After casting, the specimens were cured in a
187 controlled environment room (20°C, 40% RH) for 24 hours and then demoulded. After
188 demoulding, they were cured under water at 20°C. Specimens to be tested in an
189 uncarbonated condition were cured in water until an age of 28 days, whilst those to be
190 carbonated were removed from water at an age of 14 days and placed in a carbonation
191 chamber for a further 28 days.

192 To determine the effect of carbonation on the hydration products, particularly the mass of
193 calcium hydroxide and calcium carbonate, thermogravimetric analysis (TGA) and X-ray
194 powder diffraction (XRD) were carried out on paste samples. All pastes matched the mix
195 ratios given in Table 1 subject to the elimination of the sand. Duplicate paste samples were
196 made with one cured in water and the other subject to the carbonation regime.

197

198 **2.6 Test methods**

199 ***2.6.1 Isothermal conduction calorimetry***

200 To investigate the effect of self-healing agents on the hydration of cement, isothermal
201 conduction calorimetry tests were conducted using a Calmetrix I-cal 4000. All tests were
202 carried out on mortar samples at 20°C. Mix proportions of mortar samples were in the same
203 proportions as given in Table 1.

204

205 ***2.6.2 Carbonation***

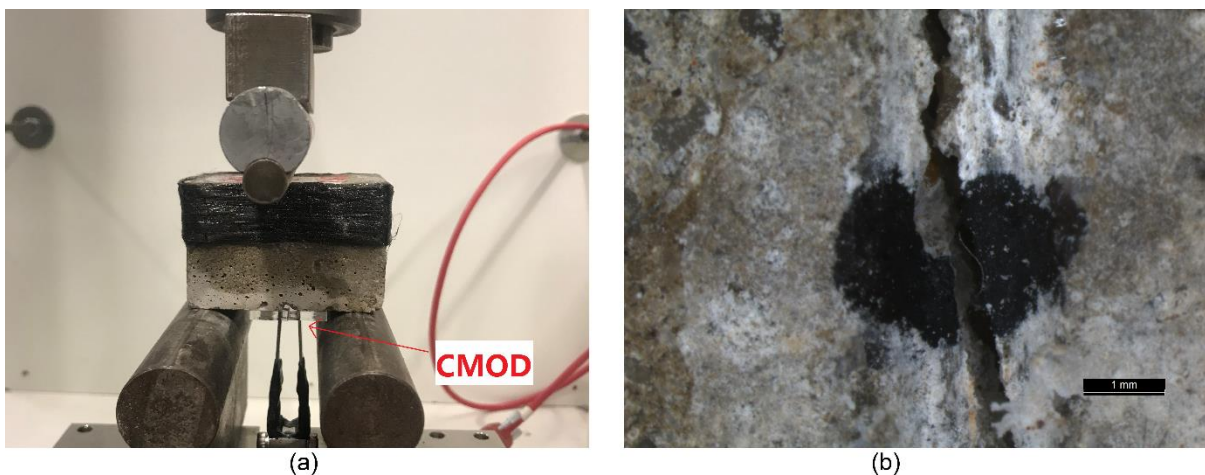
206 After 14 days of curing, selected mortar and paste specimens were placed in a carbonation
207 chamber with a CO₂ concentration of 20% and relative humidity of 50% for 28 days. To
208 evaluate the effectiveness of the carbonation method, thermogravimetric analysis (TGA) was
209 carried out using a Setsys Evolution TGA 16/18 instrument on the hardened pastes. 20 mg
210 of hardened paste was placed in an alumina crucible and heated from 30 to 1000°C at a rate
211 of 10°C/minute under 50 ml/minute flow of inert nitrogen gas.

212

213 **2.6.3 Crack creation**

214 After 28 days the specimens were dried at room temperature for 24 hours. The top third of
215 the prisms was wrapped with carbon fibre reinforced polymer strips to enable a controlled
216 width crack to be generated. Specimens were subjected to cracking using three-point
217 bending using a 30 kN Instron static testing frame over a span of 60 mm with the load
218 applied at the centre point (Figure 2(a)) to generate a crack through the lower part of the
219 prisms containing the healing agents. Crack opening was measured using a crack mouth
220 opening displacement (CMOD) gauge. A notch of approximately 1.5 mm depth was sawn at
221 mid-span to serve as an initiation point to cracking. Load was applied to maintain a crack
222 growth of 20 μm per minute. Loading was stopped when the crack width was sufficiently
223 large (~ 1 mm) that it could be expected to be approximately 500 μm wide on removal of the
224 load after allowing for elastic rebound. Selected parts of the crack were marked with a
225 permanent marker pen (Figure. 2(b)) to facilitate the monitoring of crack healing using an
226 optical microscope.

227



228

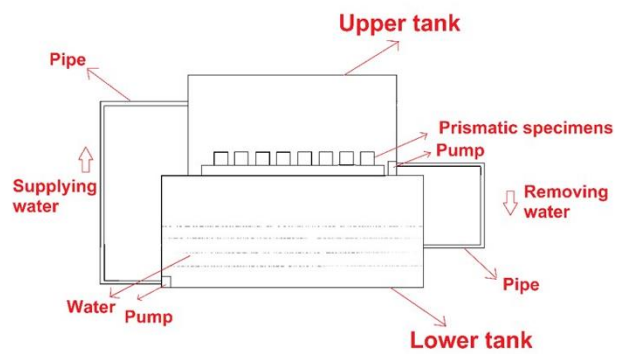
229 *Figure 2 Creation of cracks in hardened mortar, (a) three-point bending set-up, (b) marked crack*

230

231 **2.6.4 Healing**

232 Following cracking, all prisms were subjected to the healing regime. Prisms were placed in a
233 plastic tank container and supported 10 mm above the base to permit water to flow around
234 all sides. The tank was kept open to the atmosphere during the incubation period at 20°C. A

235 wet-dry cycle of 16 hours wet and 8 hours dry was used. The system used is shown in
 236 Figure 3, in which two external pumps automatically released water from the lower tank
 237 (during the wetting period) and drained water from the upper tank during the drying period.



(a)

(b)

238
 239 *Figure 3 Wet-dry healing regime, (a) on site, (b) schematic image*

240

241 **2.6.5 Investigation of self-healing efficiency**

242 ***Visualisation of crack-filling***

243 Visualisation of crack filling was performed using a Leica M205C light microscope. Images
 244 were taken of freshly cracked samples after 7, 14, 28, 56 and 84 days of healing to
 245 determine the crack width. The same part of the crack was observed every time.

246 Healing ratios (R_w) were calculated based on Equation 1:

247

248
$$R_w = \frac{w_0 - w_1}{w_0} \times 100\%$$
 Equation 1

249

250 where W_0 was the initial crack width immediately after cracking and W_1 was the crack width
251 after healing.

252 **Water flow**

253 The progressive improvement in water-resisting properties of the mortar as the crack healed
254 was determined using a water-flow test. Tests were carried out immediately after cracking
255 and after 28 days of healing. The water-flow test was based on RILEM Test Method 11.4
256 [28]. The set-up of the water-flow test is shown in Figure 4, and the water-flow coefficient, K ,
257 was calculated by Equation 2 [29].

258

$$259 \quad K = \frac{aL}{At} \ln \left[\frac{h_1}{h_2} \right] \quad \text{Equation 2}$$

260

261 Where K is the water-flowing coefficient (cm/s); a is the cross-sectional area of the pipette
262 (cm²). L is the thickness of specimen (cm); A is the cross-sectional area of specimen which
263 equals the cross-sectional area of acrylic plate (cm²); t is the time (s); h_1 is the initial water
264 head (cm); h_2 is the final water head (cm).

265

266 Healing ratios (R_K) were calculated based on Equation 3:

267

$$268 \quad R_K = \frac{K_0 - K_1}{K_0} \times 100\% \quad \text{Equation 3}$$

269

270 where K_0 was the water flow coefficient after cracking and K_1 was the water flow coefficient
271 after healing.

272

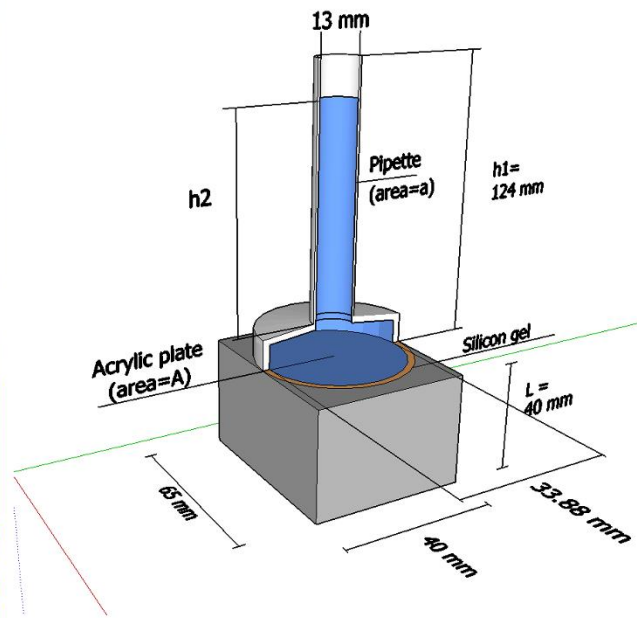
273 **2.6.6 Analytic investigation**

274 Selected and representative specimens were visualised under a scanning electron
275 microscope (SEM) after 90 days healing. These were placed in a E306 Edward Vacuum
276 Coating System until samples had outgassed. A Jeol JSM-6480LV scanning electron

277 microscope was used to obtain the image, and a backscattered image technique was used
278 at 10 kV, in which images were obtained in low vacuum and no coating was required.
279 Energy dispersive X-ray detection (EDX) was conducted at the same time as SEM to detect
280 the element composition of the healing product. A comparative element analysis was
281 conducted on the surface more than 15 mm from the crack, to aid in identification of the
282 differences between healing products and the cement hydration products.
283
284



(a)



(b)

285
286 *Figure 4 Water flow test, (a) on site set-up, (b) schematic image*
287

288 3. RESULTS

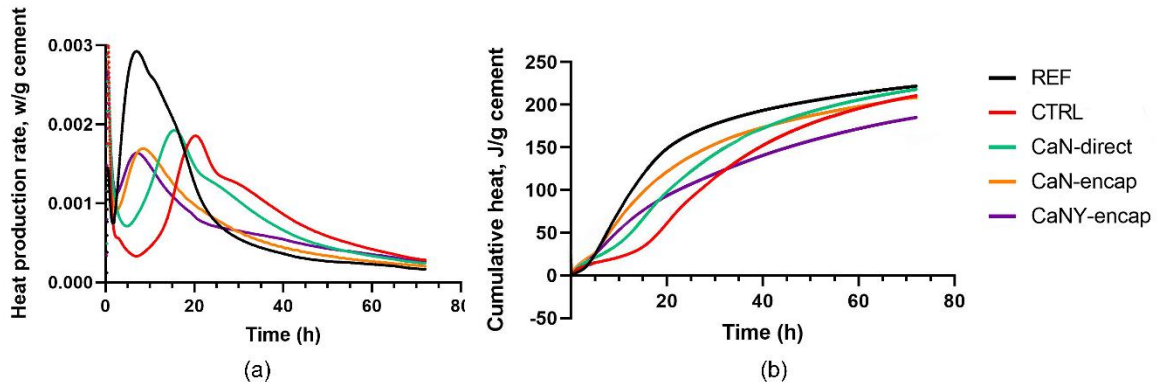
289 3.1 Kinetics of hydration

290 The kinetics of hydration of the five pastes are shown in Figure 5(a). The REF paste showed
291 typical behaviour of a CEM II/L-A paste and had a maximum rate of heat production at
292 around seven hours and a small secondary peak at approximately 10 hours. For the CTRL
293 paste, where calcium nitrate and yeast extract were added directly, a substantial delay in
294 hydration was seen, with a much longer dormant period and the maximum rate of heat
295 production occurring as late as 20 hours after the addition of water to the cement. For CaN-
296 direct paste, where the only difference to the CTRL paste was the addition of encapsulated
297 spores, a similar trend was recorded. These delays in hydration are most likely due to the
298 inclusion of the yeast extract and the presence of sugars, as has been noted elsewhere
299 [30,31].

300 However, in the two pastes where calcium nitrate and yeast extract were encapsulated in
301 ACG prior to adding them to the paste (CaN-encap or CaNY-encap), there was no
302 noticeable delay in hydration. Both of these samples had maximum rates of heat production
303 at around seven hours, the same as the REF paste. From this it can be concluded that the
304 encapsulation of the GM in ACG and then coating this with PVA was sufficient to prevent
305 leaching of GM during mixing. However, it should be noted that the maximum rate of heat
306 production was smaller at approximately 1.5 mW/g compared to 2.9 mW/g for the REF
307 paste. It is not clear why this was the case.

308 Figure 5(b) shows the cumulative heat production. Although the CTRL and CaN-direct
309 pastes were retarded, the total heat produced at around 72 hours was similar to the REF
310 paste suggesting that similar levels of cement hydration have been achieved. Overall,
311 CaNY-encap had the lowest total heat at 72 hours.

312



313

314 *Figure 5 Kinetics of hydration, (a) heat production rate, (b) cumulative heat*

315

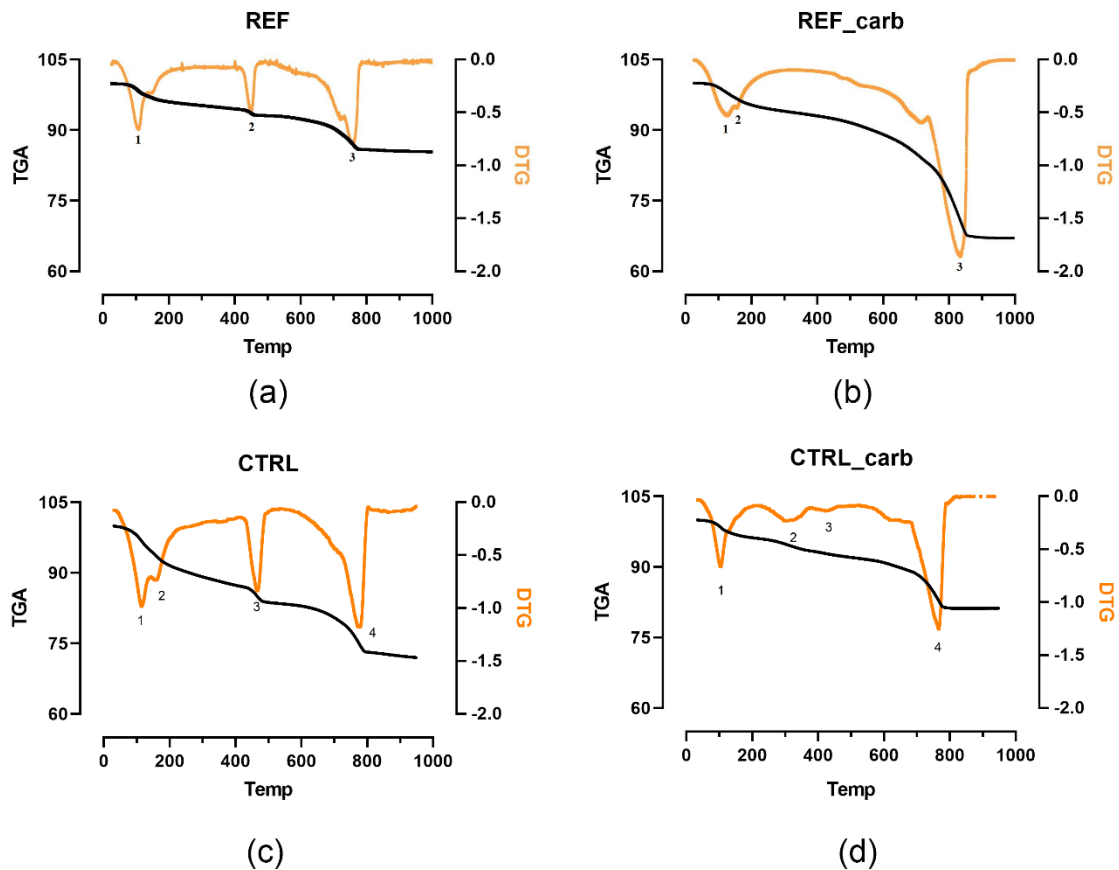
316 **3.2 Carbonation**

317 Thermal gravimetric analyses (TGA) and differential thermal gravimetric analysis (dTG) of
 318 the REF and CTRL pastes before and after carbonation are shown in Figure 6. The figures
 319 show three main troughs: Trough 1 is associated with loss of water attached to hydration
 320 products and gypsum, trough 2 is associated with the decomposition of calcium hydroxide to
 321 CaO and H₂O, whilst trough 3 is primarily related to the decomposition of calcium carbonate
 322 to CaO and CO₂. From the TGA curves it can be calculated that, at 28 days, the calcium
 323 hydroxide content of the REF paste was approximately 5% by mass, and that after
 324 carbonation it was approximately zero. For the CTRL paste, the calcium hydroxide was 20%
 325 by mass in the uncarbonated form (reflecting the direct addition of calcium nitrate and its
 326 dissolution to form calcium hydroxide), but again no calcium hydroxide was recorded after
 327 carbonation.

328 XRD was carried out on selected specimens before and after carbonation. The results are
 329 available in supplementary material. Overall, these results confirmed that the carbonation
 330 regime was particularly aggressive and consequently the resulting carbonated mortars were
 331 equivalent to mature mortars that have been exposed to XC3/XC4 environments.

332

333



334

335 *Figure 6 TGA and DTG results of (a) REF, (b) carbonated REF, (c) CTRL and (d) carbonated CTRL pastes*

336

337 3.4 Healing

338 3.4.1 Crack closure

339 The crack size of each mortar was measured using a microscope immediately after cracking
 340 and then after 7, 14, 28, 56 and 84 days of healing. The mean initial and final crack widths
 341 (84-days) are given in Table 2. Figure 7 shows the crack closure (healing) in terms of the
 342 healing ratio (R_w) with time.

343 Based on the crack size results, the bacteria-based specimens (except for CaN-encap)
 344 showed greater overall healing for both uncarbonated and carbonated specimens.
 345 Uncarbonated CaN-direct showed a higher degree of crack closure than CaN-encap. The
 346 opposite trend was seen in carbonated samples, with the CaN-encap and CaNY-encap having
 347 higher healing ratios than CaN-direct. CaNY-encap performed the best in carbonated samples,
 348 with a healing ratio of 76%. This suggests that the additional yeast extract contributed to the

349 self-healing in these specimens. While the smaller initial crack size (0.21 mm) in the CTRL
 350 specimen may have facilitated autogenous healing, the degree of healing observed in this
 351 sample was still less than that seen in all specimens containing bacteria.

352

353 Table 2 Mean values of initial (Wo) and final crack size of all mortars and healing ratio (RW)

Specimens	Uncarbonated			Carbonated		
	Initial crack size (mm)	84-days healed crack size (mm)	Healing ratio (%)	Initial crack size (mm)	84-days healed crack size (mm)	Healing ratio (%)
REF	0.38	0.38	0	0.49	0.49	0
CTRL	0.21	0.04	80%	0.35	0.35	0
CaN-direct	0.52	0.01	98%	0.38	0.32	15%
CaN-encap	0.52	0.10	81%	0.36	0.24	33%
CaNY-encap	0.43	0.00	100%	0.35	0.09	76%

354

355

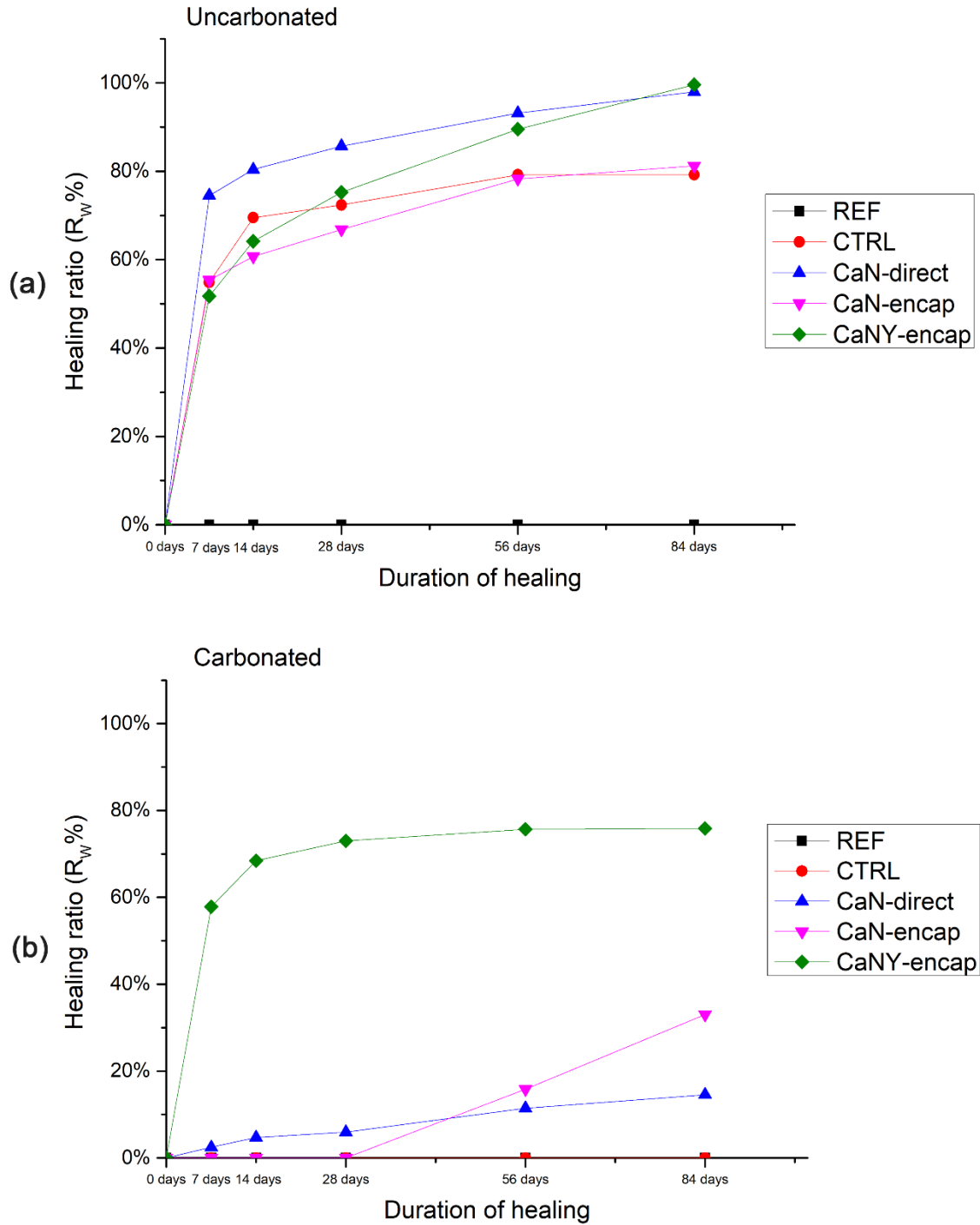
356 In addition to determining crack widths, crack closure was monitored visually over 84 days of
 357 healing using an optical microscope. Figure 8 shows the initial and final appearance (after 84
 358 days) of each mortar for both uncarbonated and carbonated conditions.

359 In uncarbonated mortars, the REF mortars showed no crystal formation within the crack,
 360 which suggested that no autogenous healing took place. On the other hand, the CTRL
 361 mortars appeared to be almost completely closed after 28 days. Reasons for this are
 362 discussed later.

363 The mortars containing bacteria showed more rapid healing. CaN-direct presented rapid
 364 precipitation on both faces of the crack after 14 days, while CaN-encap and CaNY-encap
 365 showed complete crack closure after 7 days. The healing products in mortars that were
 366 uncarbonated prior to cracking presented a consistent morphology of large and white
 367 crystals.

368 In carbonated mortars, the REF and CTRL mortars showed no evidence of self-healing.
 369 Whilst a few crystals were observed on the crack face of CaN-direct mortars, crack closure
 370 was minimal. For the CaN-encap mortar, some transparent thread-like products formed in
 371 the crack in the first 56 days, but again crack closure was low (33%). However, for the
 372 CaNY-encap mortar translucent, gel-like products formed within the crack. These products

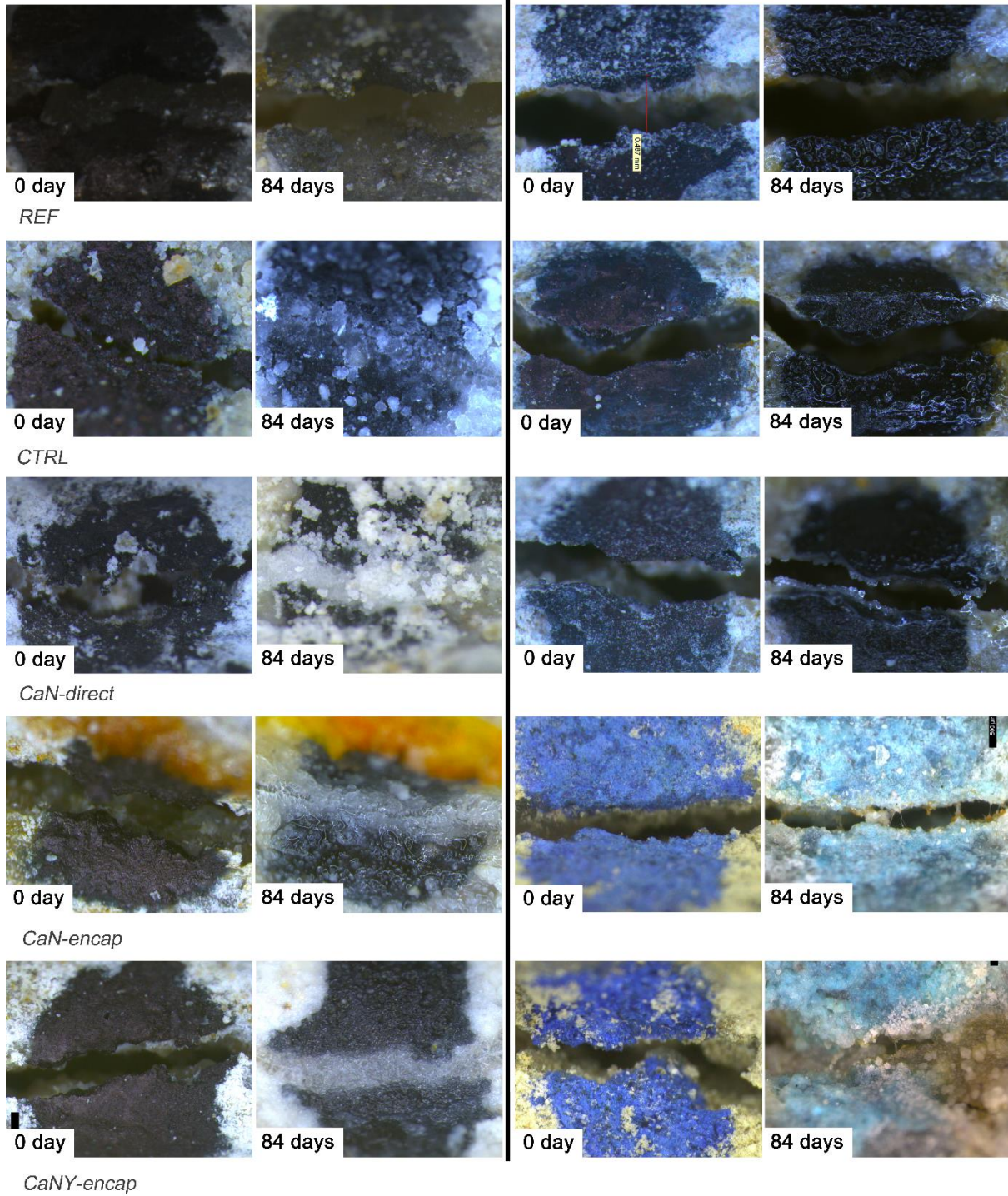
373 formed quicker than those of CaN-encap, and the degree of crack closure was significant
 374 (76%). Cracks in the CaNY-encap mortar were shown to be completely covered by the gel-
 375 substance after 28-days healing. However, after 84 days the gel-substance disappeared and
 376 crystal precipitates were present within the crack, maintaining the degree of crack closure.



377 Figure 7 Crack width healing for (a) uncarbonated mortars and (b) carbonated mortars
 378

Uncarbonated

Carbonated



379

380 *Figure 8 Progression of crack healing in images of each mortar*

381

382 **3.4.2 Water flow**

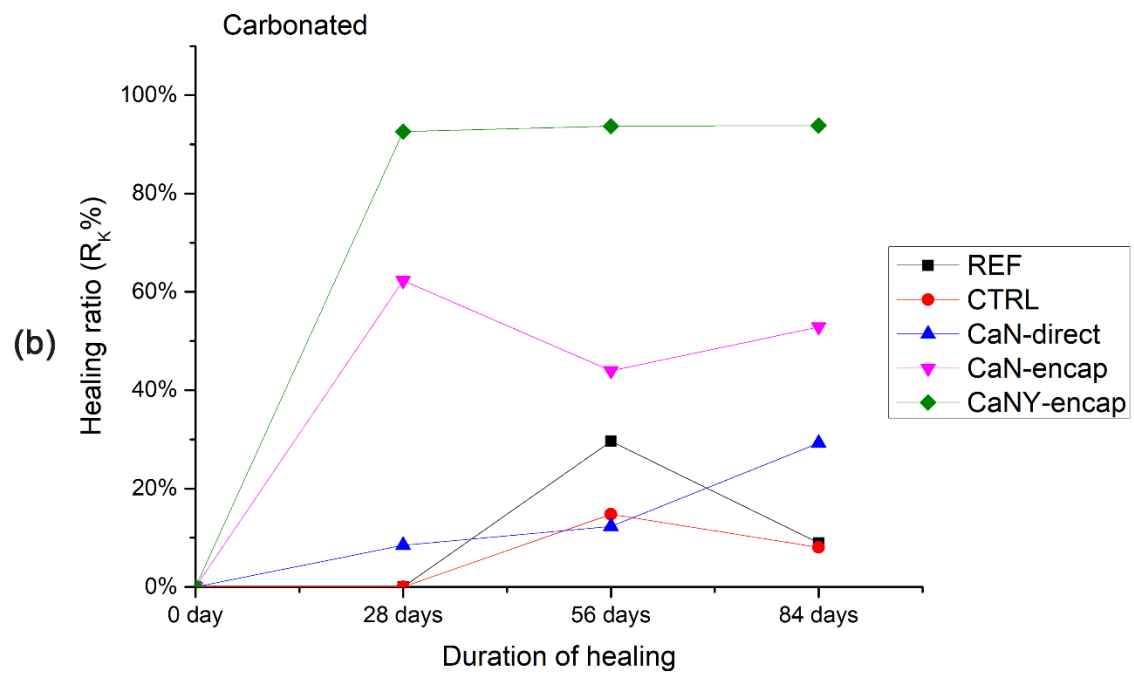
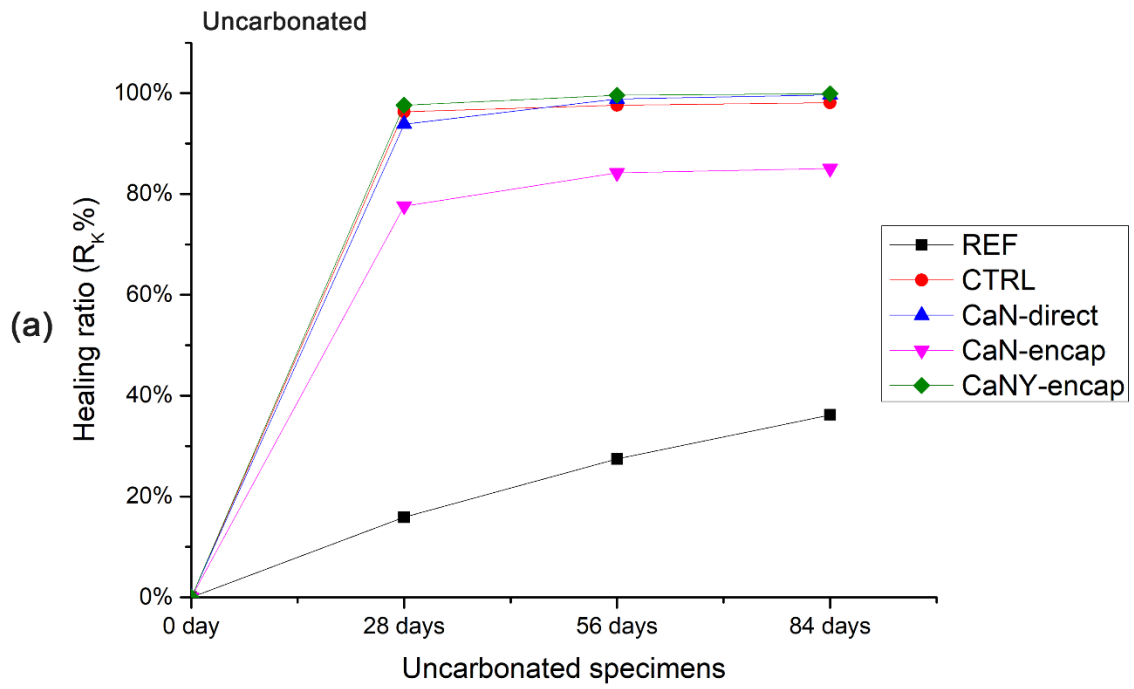
383 Water flow tests were conducted in parallel to the optical microscopy to determine the water
384 movement through the mortars as an indication of how effectively the healing mitigated
385 migration of aggressive substances through the cracked surface. Tests during the healing
386 period were conducted at 28, 56 and 84 days. Initial water flow upon cracking and final water
387 flow after 84 days of healing are given in Table 3. The healing ratio of each mortar compared
388 to the water-flow is shown in Figure 9. These results were generally consistent with the
389 microscopy and measurements of crack closure.

390 For the uncarbonated mortars (Figure 9a), REF showed only a slight decrease in water flow
391 coefficient after healing (from 0.056 cm/s to 0.036 cm/s), whereas other mortars showed
392 significant reductions in water flow coefficient and therefore higher R_k values. CaNY-encap
393 gave the highest reduction in water flow, followed by CaN-direct. It was noted that the CTRL
394 specimen gave better resistance to water flow after healing than CaN-encap, despite having
395 similar levels of crack width closure ($R_w \approx 80\%$). This is most likely due to the much lower
396 average crack width of the CTRL mortars such that after 80% crack closure CTRL mortars
397 had an average crack width of 0.04 mm compared to 0.10 mm wide in CaN-encap.

398 For the carbonated specimens, the REF, CTRL and CaN-direct mortars did not show any
399 significant reduction in water flow after the healing period (Figure 9b). However, the
400 encapsulated specimens showed a different trend, which was consistent with crack closure.
401 The carbonated CaN-encap mortars had a healing ratio of 60% after 28 days, which fell to
402 around 50% at 84 days. For CaNY-encap mortars the healing ratio was over 90% at 28 days
403 and this was maintained at 84 days.

404

405



406

407

408 *Figure 9 Healing of mortars in terms of reduction in water-flow coefficient for (a) uncarbonated mortars and (b)*
 409 *carbonated mortars*

410

411

412

413 Table 3 Mean values of initial and final water permeability coefficient of specimens

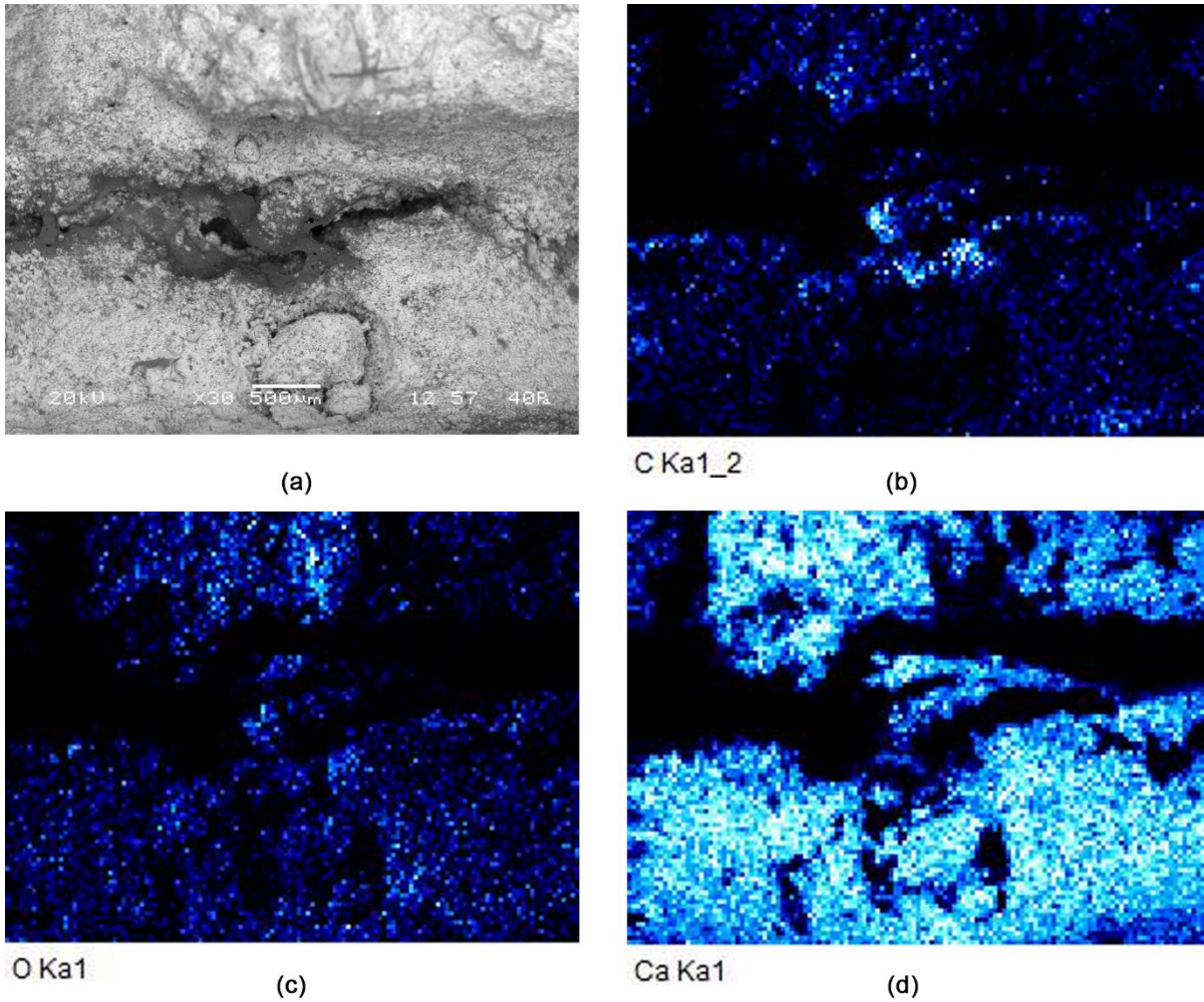
Specimens	Uncarbonated			Carbonated		
	Initial water permeability (cm/s)	Final water permeability (cm/s)	Healing ratio (R _p %)	Initial water permeability (cm/s)	Final water permeability (cm/s)	Healing ratio (R _p %)
REF	0.056	0.036	36%	0.324	0.295	9%
CTRL	0.033	0.001	98%	0.149	0.137	8%
CaN-direct	0.046	0.000	100%	0.130	0.092	29%
CaN-encap	0.244	0.004	85%	0.057	0.027	53%
CaNY-encap	0.140	0.000	100%	0.022	0.001	94%

414

415

416 **3.4.3 SEM and EDX of healing products**

417 After 90 days of healing, SEM and EDX were conducted on selected mortars. Figure 10
 418 shows element mapping analysis as applied to a cracked area of a CaNY-encap mortar. The
 419 original mortar is seen at the top and bottom Figure 10(a), and the crack runs through the
 420 centre from left to right. In general, the element mapping (Figures 10(b) to Figure 10(d))
 421 showed that the healing product contained patches of calcium products present within the
 422 crack, but seemingly not necessarily attached to the crack face. Due to the nature of the
 423 technique the values for carbon and oxygen are of limited practical application, but it does
 424 appear that the crack contains these elements. It can be suggested that the healing product
 425 is calcium carbonate. Images on other mortars are given in the supplementary information.



426

427 *Figure 10 EDX map of carbonated CaNY-encap, (a) applied area, (b) carbon distribution, (c) oxygen distribution*
 428 *and (d) calcium distribution*

429 **4. Discussion**

430 **4.1 Comparison of healing in uncarbonated and carbonated mortars**

431 **4.1.1 Mortars without bacteria**

432 The REF mortars were made with cement and sand, and no additional components. Visual
 433 observations showed no healing of the REF mortars for either the uncarbonated or
 434 carbonated conditions. This observation shows that the mortars were sufficiently hydrated
 435 after 28 days and that no autogenous healing could take place at the surface. The small
 436 recovery in water penetration may represent some autogenous healing deep within the
 437 crack. The inability of autogenous healing to occur at the surface in the REF mortars,
 438 enables us to determine that all surface healing in other mortars was due to either the

439 inclusion of GM, bacterial activity or a combination of both, and was not due to natural
440 carbonation processes during the wetting/drying healing period.

441 The CTRL specimens contained calcium nitrate and yeast extract directly added to the
442 mortars. Here it was shown that for the uncarbonated mortars there was observable healing
443 at the surface and a good recovery of the water penetration properties. However, the cracks
444 formed in these specimens were smaller than those in other mortars and this may have
445 facilitated healing and it should not be considered that healing would have been of the same
446 degree had the cracks been closer to 0.4 to 0.5 mm in width. When cracks were formed after
447 carbonation, visual observations showed no healing for the CTRL mortars. This suggests
448 that the availability of calcium hydroxide in the uncarbonated mortars must be key in
449 ensuring the autogenous self-healing observed. Clearly, as shown through TGA (Figure 9)
450 the direct addition of calcium nitrate led to greater quantities of calcium hydroxide in the
451 uncarbonated mortars. It is likely that this calcium hydroxide acted as the source of Ca^{2+} ions
452 for effective healing when required. This excess of calcium hydroxide may have aided
453 healing via natural carbonation during the wet/dry healing period. However, as described
454 above, the fact that the REF mortar showed no autogenous healing at the surface at all,
455 despite the availability of some calcium hydroxide, means we can reject this hypothesis.
456 Consequently, it is postulated that the yeast extract allowed some of the environmental
457 bacteria in the healing water to grow in the cracks and that this has led to healing.

458

459 **4.1.2 Bacteria-based self-healing mortars with direct addition of GM**

460 The CaN-direct mortars used in this research contained spores of *B. cohnii* encapsulated in
461 ACG with the GM added directly to the matrix. It was observed that for these mortars, those
462 that were not carbonated before they were cracked, healed well – both visually in terms of
463 crack reduction (100% crack closure at 84 days) and in recovery of water penetration
464 properties. However, when cracks were formed after carbonation the degree of healing was
465 poor; with only 10% crack closure at 84 days.

466 For autonomous bacteria-based self-healing to occur in these mortars, Ca^{2+} ions need to be
467 attracted to the surface of the bacteria. As discussed previously, and as for the CTRL
468 specimens, the most accessible form of Ca^{2+} ions is most likely to be calcium hydroxide.
469 Since there was no calcium hydroxide present in the carbonated mortars this explains why
470 healing did not occur. Consequently, it appears that the direct addition of calcium nitrate to
471 mortar is not a practicable means of obtaining self-healing in concrete that is likely to
472 carbonate before it cracks because the Ca^{2+} ions become locked in a form that is
473 insufficiently soluble for the bacteria to use. This observation has not been noted in previous
474 research.

475 Nevertheless, that these mortars healed well in uncarbonated conditions remains a positive
476 finding. Indeed, it was observed that in the uncarbonated mortars the degree of healing was
477 similar if not better than the degree of healing observed when GM was included in the mortar
478 in an encapsulated form (discussed below). This suggests that sufficient Ca^{2+} was formed
479 within the vicinity of the crack for precipitation of calcium carbonate to take place and
480 consequently it can be argued that the direct addition of GM is a suitable option for self-
481 healing when concrete will not be subject to significant carbonation over its life-time.

482

483 ***4.1.3 Self-healing mortars with encapsulated GM***

484 In both CaN-encap and CaNY-encap the GM was encapsulated in ACG. This prevented the
485 calcium nitrate, therein, from reacting with water to form calcium hydroxide before any
486 cracking occurred and therefore in the carbonation environment it did not convert to calcium
487 carbonate.

488 It was observed that for these mortars crack closure and a recovery of water-flow resisting
489 properties was observed under both uncarbonated and carbonated conditions. CaN-encap
490 had healing of 81% (crack closure) in uncarbonated conditions and 33% (crack closure) in
491 carbonated conditions; whilst CaNY-encap had a healing ratio of 100% in uncarbonated
492 conditions and 76% in carbonated conditions (Table 2). A similar trend in terms of self-
493 healing capability was observed in the water flow test results (Table 3).

494 From the observations on the carbonated mortars and comparison with the mortars where
495 GM was added directly (CaN-direct), it can be reasoned that the source of Ca^{2+} ions in these
496 mortars was the encapsulated calcium nitrate. The ability of these mortars to self-heal was
497 related only to the ability of the ACG to fracture and release the GM (calcium nitrate and
498 yeast extract) at the location of the crack. However, noticeably the degree of healing was
499 less than that in uncarbonated mortars. This suggests that in uncarbonated mortars, calcium
500 hydroxide generated by the hydration of cement is also utilised by the bacteria for healing
501 purposes.

502 It should be noted that after carbonation, the “healing” product at the surface of CaN-encap
503 and CaNY-encap mortars had a gel-like status, and differed from what occurred in the
504 uncarbonated mortars. The most likely explanation is that these gel-like phases are bacterial
505 biofilm or a by-product of the growth of the bacterial cells. This biofilm was mainly formed in
506 the first two months but disappeared by 84 days. Some large crystal precipitates were
507 shown to fill the crack after the disappearance of the biofilm. Based on the water flow test
508 results, and the fact that CaN-encap and CaNY-encap had good recovery of water-flow
509 resistance it is most likely that calcium carbonate was precipitated on the biofilm, providing
510 sufficient healing performance. More of this gel-like formation was observed in the CaNY-
511 encap mortars. This makes sense, because CaNY-encap contained four times as much
512 yeast extract as CaN-encap, would support a marked increase in bacterial biomass and
513 could easily lead to more biofilm formation. The high content of calcium detected by EDX
514 mapping in the area between the original crack surface and the black gel-like healing
515 material suggested that calcite was precipitated here. The most likely explanation for this
516 arrangement is that a bacterial biofilm may form the first layer of the healing process in
517 carbonated CaNY-encap mortars, providing a scaffold and nucleation surface on which
518 calcite can precipitate over time, leading to robust and complete crack healing.

519

520 **4.1.4 Summary of effect of carbonation on self-healing of mortars**

521 Overall these results make clear that an important source of Ca^{2+} ions for bacteria-based
522 self-healing of cementitious composites is calcium hydroxide, present either as a
523 consequence of hydrolysis or hydration of Portland cement, or from the dissolution of
524 calcium nitrate deliberately added to the cementitious composite during mixing. For
525 cementitious composites that do not carbonate prior to cracking, this calcium hydroxide is
526 sufficient to provide an efficient level of healing. We note that supplying an extra source of
527 Ca^{2+} ions at the moment of cracking, due to encapsulation, enhanced the degree of healing.
528 However, in carbonated cementitious composites calcium hydroxide is not available as a
529 source of Ca^{2+} ions. We here show for the first time that the self-healing of cementitious
530 composites that crack after carbonation is almost totally dependent on the availability of Ca^{2+}
531 ions released from an encapsulated source. Therefore, whilst the direct addition and
532 encapsulation of calcium nitrate are both suitable for providing self-healing of cementitious
533 composites, the conditions of the concrete during service life need to be considered when
534 choosing the most appropriate option. For cementitious composites exposed to XC
535 conditions it is suggested that the calcium source must be encapsulated in the mortar prior
536 to mixing.

537

538 **4.2 Effect of yeast extract content on self-healing**

539 To ensure sufficient DIC, a carbon source was added to the mortars to aid bacteria-based
540 self-healing. In this research, yeast extract alone was used as the source of DIC to deliver
541 bacteria-based self-healing, something that had not been tried previously.

542 It was observed that all mortars containing bacteria and yeast extract healed when subject to
543 uncarbonated conditions prior to cracking. Consequently, the results of this work are clear in
544 that yeast extract was able to provide sufficient DIC for the bacteria to promote the
545 precipitation of calcium carbonate.

546 In both uncarbonated and carbonated mortars it was shown that CaNY-encap was more
547 effective at providing crack closure and recovery of water flow properties than CaN-encap.

548 The only difference between these two mortars was in the quantity of yeast extract added,
549 and in the tests described, yeast extract was the only nutrient source used to aid spore
550 germination and bacterial growth. Since the yeast extract was consumed by the bacteria, its
551 availability diminished with time. It can be deduced that, because CaNY-encap contains a
552 greater quantity of yeast extract, growth of bacteria can take place over a much longer
553 period.

554 Whilst yeast extract was the principle source of DIC, under the wet/dry healing conditions
555 used it is possible that some environmental CO₂ may have ingressed into the mortar.

556 However, since the quantity of DIC is directly related to the amount of CO₃²⁻ ions formed, it
557 remains that the volume of calcium carbonate precipitated is necessarily related to the
558 availability of yeast extract. This may at first glance appear a fairly obvious observation;
559 however research elsewhere has shown that too much yeast extract can inhibit calcium
560 carbonate precipitation [32]. However, unlike in the work described here, the yeast extract
561 there was used in combination with other sources of DIC.

562

563 **5 Conclusions**

564 This research has shown that an important source of Ca²⁺ ions for bacteria-based self-
565 healing of cementitious composites is calcium hydroxide. However, in carbonated
566 cementitious composites calcium hydroxide is not available as a source of Ca²⁺ ions.

567 Consequently, we have shown here for the first time, that bacteria-based self-healing, in
568 cementitious composites that have carbonated prior to cracking, is almost totally dependent
569 on the availability of Ca²⁺ ions released from an encapsulated source.

570 The following specific conclusions can be drawn:

- 571 1. Coated ACG is an effective medium for encapsulating spores and GM in bacteria-
572 based self-healing cementitious composites. It survives the mixing and hardening
573 process intact, causes no retardation and fractures when cracks are formed.

- 574 2. Uncarbonated mortars show higher self-healing efficiency than carbonated mortars.
575 Calcium carbonate precipitates within approximately seven days, and complete
576 surface crack closure can be observed visually in less than a month.
- 577 3. In carbonated specimens, where healing is only observed with encapsulated GM, a
578 biofilm was observed to be formed and fill the crack for up to 84 days. Only then did
579 the precipitated calcium carbonate within the crack become visible. It is possible that
580 the formation of a bacterial biofilm contributes to early crack-healing, while calcium
581 carbonate precipitation on the surface of the biofilm over time leads to the crack
582 closure.
- 583 4. The quantity of yeast extract available for use by the bacteria governs self-healing
584 performance when bacteria are used with calcium nitrate. The quantity of calcium
585 carbonate that can form is directly related to the amount of yeast extract provided.
586

587 **ACKNOWLEDGEMENTS**

588 The authors would like to acknowledge EPSRC (Project No. EP/PO2081X/1) and Industrial
589 collaborators/partners for funding the Resilient Materials for Life (RM4L) project. We thank
590 technical staff in the Department of Architecture and Civil Engineering and the Department of
591 Biology and Biochemistry for key support. We further thank colleagues at the Material and
592 Chemical Characterisation Facility (MC²) at University of Bath
593 (<https://doi.org/10.15125/mx6j-3r54>) for their assistance with scanning electron microscopy.
594

595 **REFERENCES**

- 596 [1] A. Al-Tabbaa, B. Lark, K. Paine, T. Jefferson, C. Litina, D. Gardner, T. Embley,
597 Biomimetic cementitious construction materials for next-generation infrastructure,
598 Proc. Inst. Civ. Eng. - Smart Infrastruct. Constr. (2018) 1–35.
599 doi:<https://doi.org/10.1680/jsmic.18.00005>.
- 600 [2] A. Mignon, G.J. Graulus, D. Snoeck, J. Martins, N. De Belie, P. Dubruel, S. Van
601 Vlierberghe, pH-sensitive superabsorbent polymers: a potential candidate material for

- 602 self-healing concrete, *J. Mater. Sci.* 50 (2014) 970–979. doi:10.1007/s10853-014-
603 8657-6.
- 604 [3] M. Roig-Flores, F. Pirritano, P. Serna, L. Ferrara, Effect of crystalline admixtures on
605 the self-healing capability of early-age concrete studied by means of permeability and
606 crack closing tests, *Constr. Build. Mater.* 114 (2016) 447–457.
607 doi:10.1016/j.conbuildmat.2016.03.196.
- 608 [4] L. Souza, A. Kanellopoulos, A. Al-Tabbaa, Production of microcapsules for self-
609 healing concrete using microfluidics, in: *5th Int. Conf. Self-Healing Mater.*, Durham,
610 USA, 2015.
- 611 [5] A. Kanellopoulos, P. Giannaros, A. Al-Tabbaa, The effect of varying volume fraction of
612 microcapsules on fresh, mechanical and self-healing properties of mortars, *Constr.*
613 *Build. Mater.* 122 (2016) 577–593. doi:10.1016/J.CONBUILDMAT.2016.06.119.
- 614 [6] R.E. Davies, A. Jefferson, R. Lark, D. Gardner, A novel 2D vascular network in
615 cementitious materials, in: *Fib Symp.*, Copenhagen, Denmark, 2015.
616 <http://orca.cf.ac.uk/86643/> (accessed December 2, 2018).
- 617 [7] N. De Belie, E. Gruyaert, A. Al-Tabbaa, P. Antonaci, C. Baera, D. Bajare, A.
618 Darquennes, R. Davies, L. Ferrara, T. Jefferson, C. Litina, B. Miljevic, A. Otlewska, J.
619 Ranogajec, M. Roig-Flores, K. Paine, P. Lukowski, P. Serna, J.M. Tulliani, S. Vucetic,
620 J. Wang, H.M. Jonkers, A Review of Self-Healing Concrete for Damage Management
621 of Structures, *Adv. Mater. Interfaces.* 5 (2018) 1–28. doi:10.1002/admi.201800074.
- 622 [8] W. De Muynck, N. De Belie, W. Verstraete, Microbial carbonate precipitation in
623 construction materials: A review, *Ecol. Eng.* 36 (2010) 118–136.
624 doi:10.1016/j.ecoleng.2009.02.006.
- 625 [9] E. Tziviloglou, V. Wiktor, H.M. Jonkers, E. Schlangen, Bacteria-based self-healing
626 concrete to increase liquid tightness of cracks, *Constr. Build. Mater.* 122 (2016) 118–
627 125. doi:10.1016/j.conbuildmat.2016.06.080.
- 628 [10] S.S. Bang, J.K. Galinat, V. Ramakrishnan, Calcite precipitation induced by
629 polyurethane-immobilized *Bacillus pasteurii*, *Enzyme Microb. Technol.* 28 (2001) 404–

- 630 409. doi:10.1016/S0141-0229(00)00348-3.
- 631 [11] H. Chen, C. Qian, H. Huang, Self-healing cementitious materials based on bacteria
632 and nutrients immobilized respectively, *Constr. Build. Mater.* 126 (2016) 297–303.
633 doi:10.1016/J.CONBUILDMAT.2016.09.023.
- 634 [12] N. De Belie, J. Wang, Z.B. Bundur, K. Paine, Bacteria-based concrete, in: *Eco-
635 Efficient Repair Rehabil. Concr. Infrastructures*, Woodhead Publishing, 2018: pp.
636 531–567. doi:10.1007/978-1-4939-6881-7.
- 637 [13] B.J. Reeksting, T.D. Hoffmann, L. Tan, K. Paine, S. Gebhard, In-depth profiling of
638 calcite precipitation by environmental bacteria reveals fundamental mechanistic
639 differences with relevance to application, *Appl. Environ. Microbiol.* 86 (2020) 1–16.
640 doi:10.1128/aem.02739-19.
- 641 [14] J.Y. Wang, H. Soens, W. Verstraete, N. De Belie, Self-healing concrete by use of
642 microencapsulated bacterial spores, *Cem. Concr. Res.* 56 (2014) 139–152.
643 doi:10.1016/j.cemconres.2013.11.009.
- 644 [15] M. Luo, C.X. Qian, Performance of Two Bacteria-Based Additives Used for Self-
645 Healing Concrete, *J. Mater. Civ. Eng.* 28 (2016) 04016151.
646 doi:10.1061/(ASCE)MT.1943-5533.0001673.
- 647 [16] D. Palin, V. Wiktor, H.M. Jonkers, A bacteria-based bead for possible self-healing
648 marine concrete applications, *Smart Mater. Struct.* 25 (2016) 084008.
649 doi:10.1088/0964-1726/25/8/084008.
- 650 [17] M. Alazhari, T. Sharma, A. Heath, R. Cooper, K. Paine, Application of expanded
651 perlite encapsulated bacteria and growth media for self-healing concrete, *Constr.
652 Build. Mater.* 160 (2018) 610–619. doi:10.1016/j.conbuildmat.2017.11.086.
- 653 [18] M. Fahimizadeh, A.D. Abeyratne, L.S. Mae, R. Singh, P. Pasbakhsh, Biological
654 concrete self-healing by hydrogel- immobilized non-ureolytic bacteria, n.d.
- 655 [19] J. Xu, X. Wang, Self-healing of concrete cracks by use of bacteria-containing low
656 alkali cementitious material, *Constr. Build. Mater.* 167 (2018) 1–14.
657 doi:10.1016/J.CONBUILDMAT.2018.02.020.

- 658 [20] Z. Bařaran Bundur, S. Bae, M.J. Kirisits, R.D. Ferron, Biomineralization in Self-
659 Healing Cement-Based Materials: Investigating the Temporal Evolution of Microbial
660 Metabolic State and Material Porosity, *J. Mater. Civ. Eng.* 29 (2017) 04017079.
661 doi:10.1061/(ASCE)MT.1943-5533.0001838.
- 662 [21] J.L. Zhang, C.G. Wang, Q.L. Wang, J.L. Feng, W. Pan, X.C. Zheng, B. Liu, N.X. Han,
663 F. Xing, X. Deng, A binary concrete crack self-healing system containing oxygen-
664 releasing tablet and bacteria and its Ca²⁺-precipitation performance, *Appl. Microbiol.*
665 *Biotechnol.* 100 (2016) 10295–10306. doi:10.1007/s00253-016-7741-z.
- 666 [22] M. Ksara, R. Newkirk, S.K. Langroodi, F. Althoey, C.M. Sales, C.L. Schauer, Y.
667 Farnam, Microbial damage mitigation strategy in cementitious materials exposed to
668 calcium chloride, *Constr. Build. Mater.* 195 (2019) 1–9.
669 doi:10.1016/j.conbuildmat.2018.10.033.
- 670 [23] J.L. Zhang, R.S. Wu, Y.M. Li, J.Y. Zhong, X. Deng, B. Liu, N.X. Han, F. Xing,
671 Screening of bacteria for self-healing of concrete cracks and optimization of the
672 microbial calcium precipitation process, *Appl. Microbiol. Biotechnol.* 100 (2016) 6661–
673 6670. doi:10.1007/s00253-016-7382-2.
- 674 [24] B. řavija, M. Luković, Carbonation of cement paste: Understanding, challenges, and
675 opportunities, *Constr. Build. Mater.* 117 (2016) 285–301.
676 doi:10.1016/j.conbuildmat.2016.04.138.
- 677 [25] J. Wang, A. Mignon, D. Snoeck, V. Wiktor, S. Van Vliergerghe, N. Boon, N. De Belie,
678 Application of modified-alginate encapsulated carbonate producing bacteria in
679 concrete: a promising strategy for crack self-healing, *Front. Microbiol.* 6 (2015) 1–14.
680 doi:10.3389/fmicb.2015.01088.
- 681 [26] H.M. Jonkers, A. Thijssen, G. Muyzer, O. Copuroglu, E. Schlangen, H.M. Jonkers, A.
682 Thijssen, G. Muyzer, O. Copuroglu, E. Schlangen, Application of bacteria as self-
683 healing agent for the development of sustainable concrete, *Ecol. Eng.* 36 (2010) 230–
684 235. doi:10.1016/j.ecoleng.2008.12.036.
- 685 [27] R. Alghamri, A. Kanellopoulos, A. Al-Tabbaa, Impregnation and encapsulation of

686 lightweight aggregates for self-healing concrete, *Constr. Build. Mater.* 124 (2016)
687 910–921. doi:10.1016/j.conbuildmat.2016.07.143.

688 [28] RILEM, Measurement of Water Absorption Under Low Pressure. RILEM Test Method
689 No. 11.4, 1987.

690 [29] J.N. Cernica, *Geotechnical Engineering: Soil Mechanics*, Wiley, 1995.

691 [30] X. Chen, J. Yuan, M. Alazhari, Effect of Microbiological Growth Components for
692 Bacteria-Based Self-Healing on the Properties of Cement Mortar, *Materials (Basel)*.
693 12 (2019). doi:10.3390/ma12081303.

694 [31] A. Amiri, Z.B. Bundur, Impact of Biogenic Self-Healing Additive on Performance of
695 Cement-Based Mortar, *Int. RILEM Conf. Mater. Syst. Struct. Civ. Eng. Conf. Segm.*
696 *Serv. Life Cem. Mater. Struct.* (2016) 493–502.

697 [32] J. Zhang, B. Mai, T. Cai, J. Luo, W. Wu, B. Liu, N. Han, F. Xing, X. Deng,
698 Optimization of a Binary Concrete Crack Self-Healing System Containing Bacteria
699 and Oxygen, *Materials (Basel)*. 10 (2017) 116. doi:10.3390/ma10020116.

700

701

702 **Supplementary documents:**

703

704 1. XRD

705 2. Crack closure progression photos

706 3. SEM and EDX images across cracks of selected mortars

707

708
709
710
711
712
713
714
715
716
717
718
719
720
721
722
723
724
725
726

1. XRD

An accelerated carbonation method was used in this work to convert the calcium hydroxide formed during the hydrolysis and hydration of cement to calcium carbonate prior to cracking to test the effects of this on self-healing. As shown by the TGA and XRD results this was successful and after carbonation there was no calcium hydroxide present in either the REF or CTRL mortars.

The analyses show some items of interest. Firstly, there was no evidence of ettringite in the carbonated REF mortars. Ettringite is known to carbonate to form calcium carbonate, gypsum ($\text{CaSO}_4 \cdot 2\text{H}_2\text{O}$), alumina gel ($\text{Al}_2\text{O}_3 \cdot \text{H}_2\text{O}$) and water [31]. Indeed, the presence of gypsum in carbonated REF mortars was identified. In contrast, the quantity of ettringite in the carbonated CTRL mortars was similar to the uncarbonated mortar and no gypsum was formed. This may be because the addition of calcium nitrate caused an increase in calcium hydroxide content, and subsequently during the timeframe of the carbonation period CO_2 was largely consumed by calcium hydroxide

Figure S1 shows the XRD results of uncarbonated and carbonated REF and CTRL paste samples.

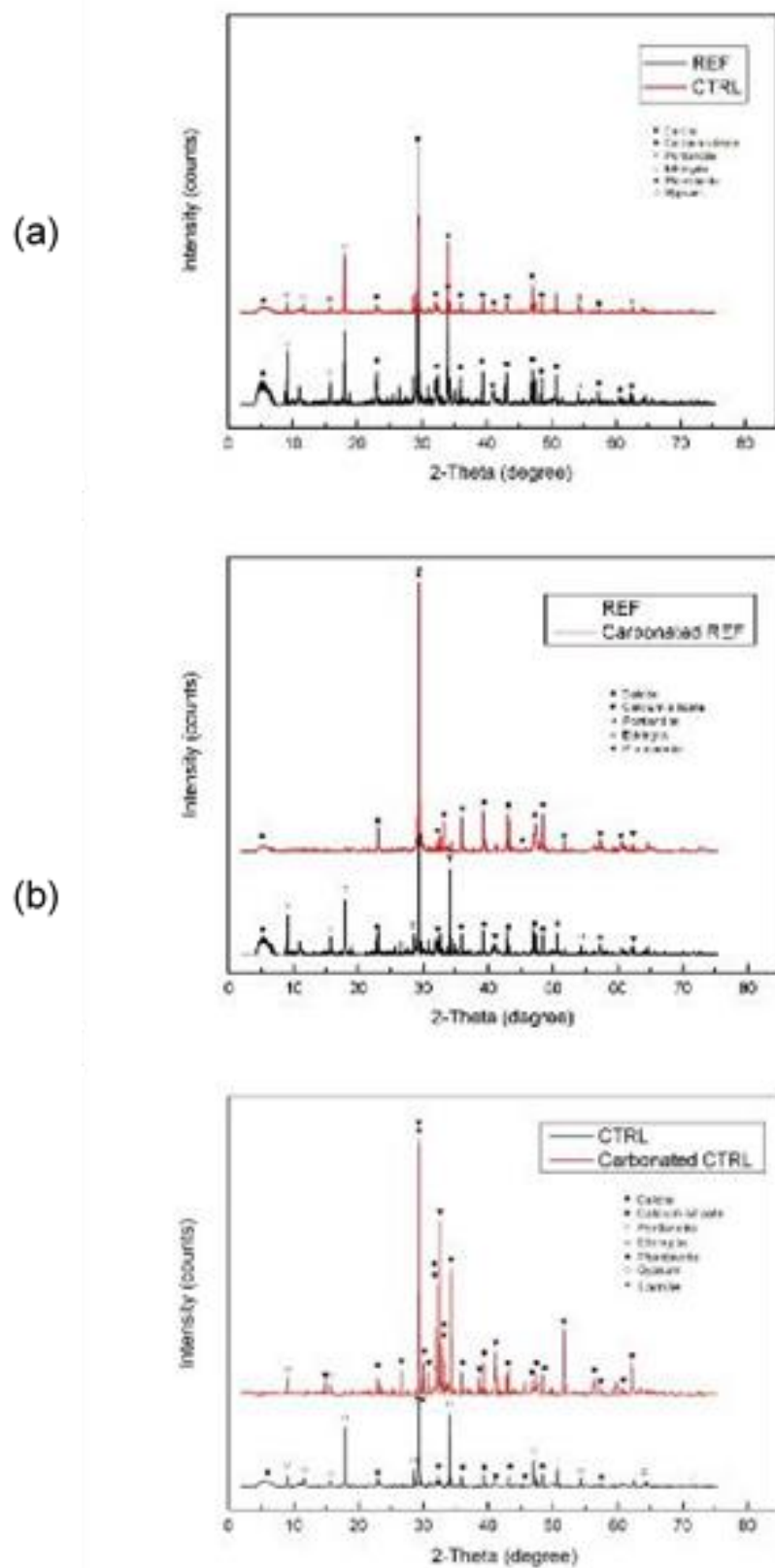


Figure S1 XRD results of (a) REF & CTRL, (b) REF & carbonated REF and (c) CTRL and carbonated CTRL

728

729 **2. Crack Closure Progression**

730 Progression photos of crack healing of each mortar are shown in Figure S2-6

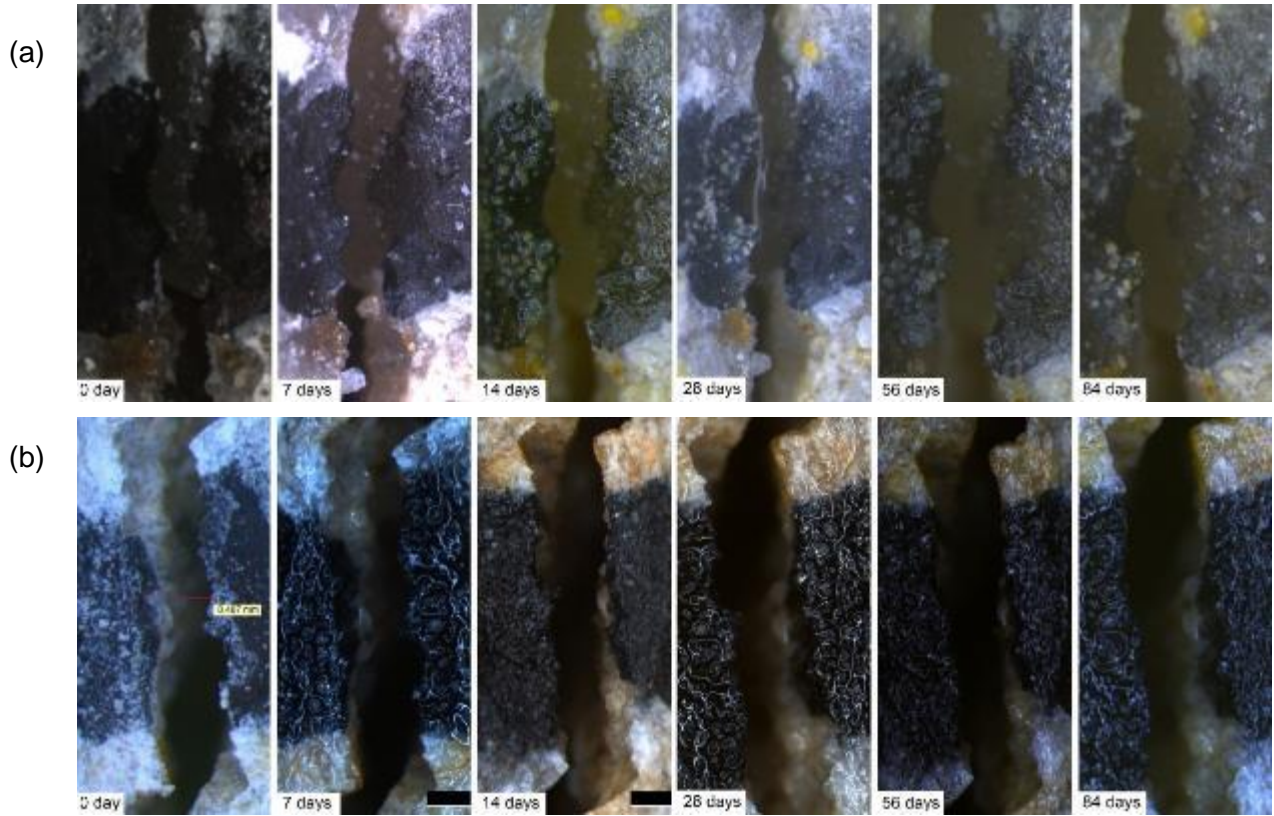


Figure S3 Progression of crack healing in (a) REF and (b) carbonated REF

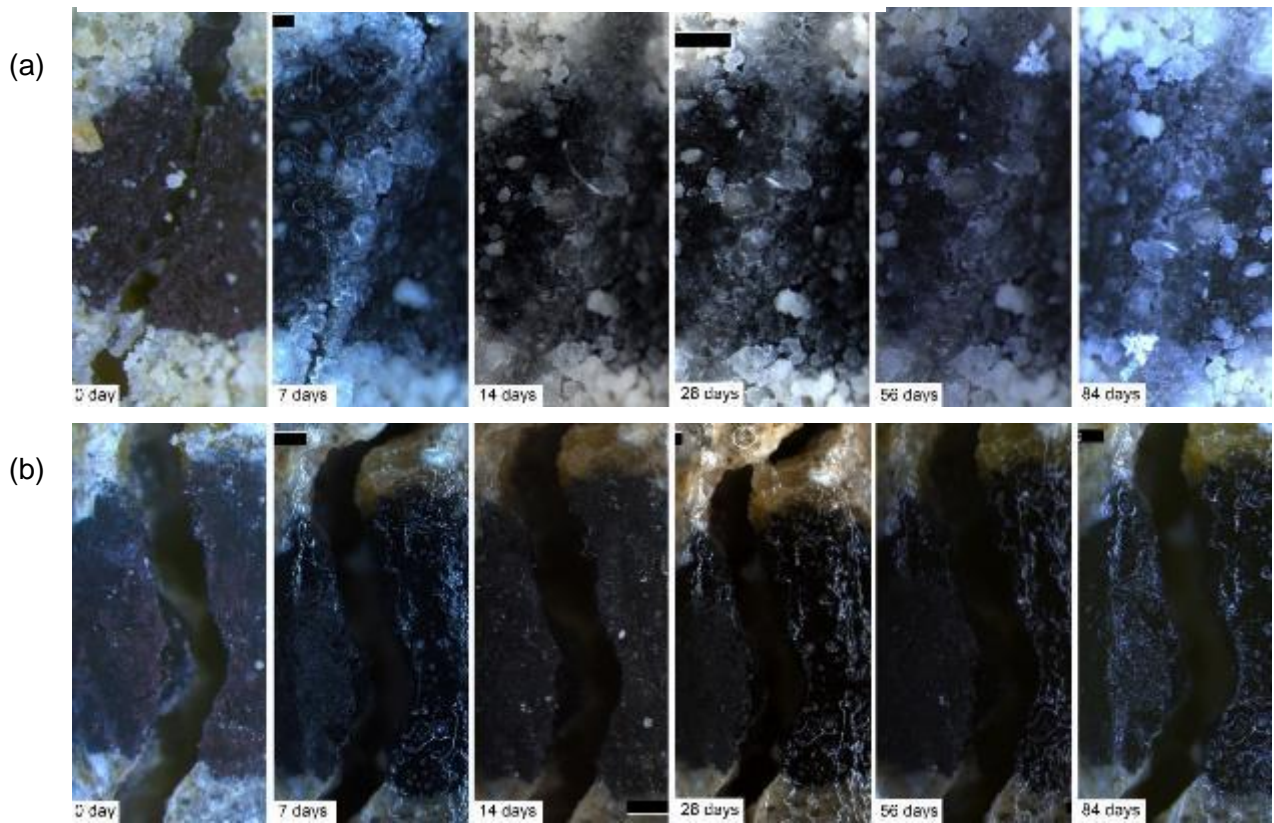


Figure S2 Progression of crack healing in (a) CTRL and (b) carbonated CTRL

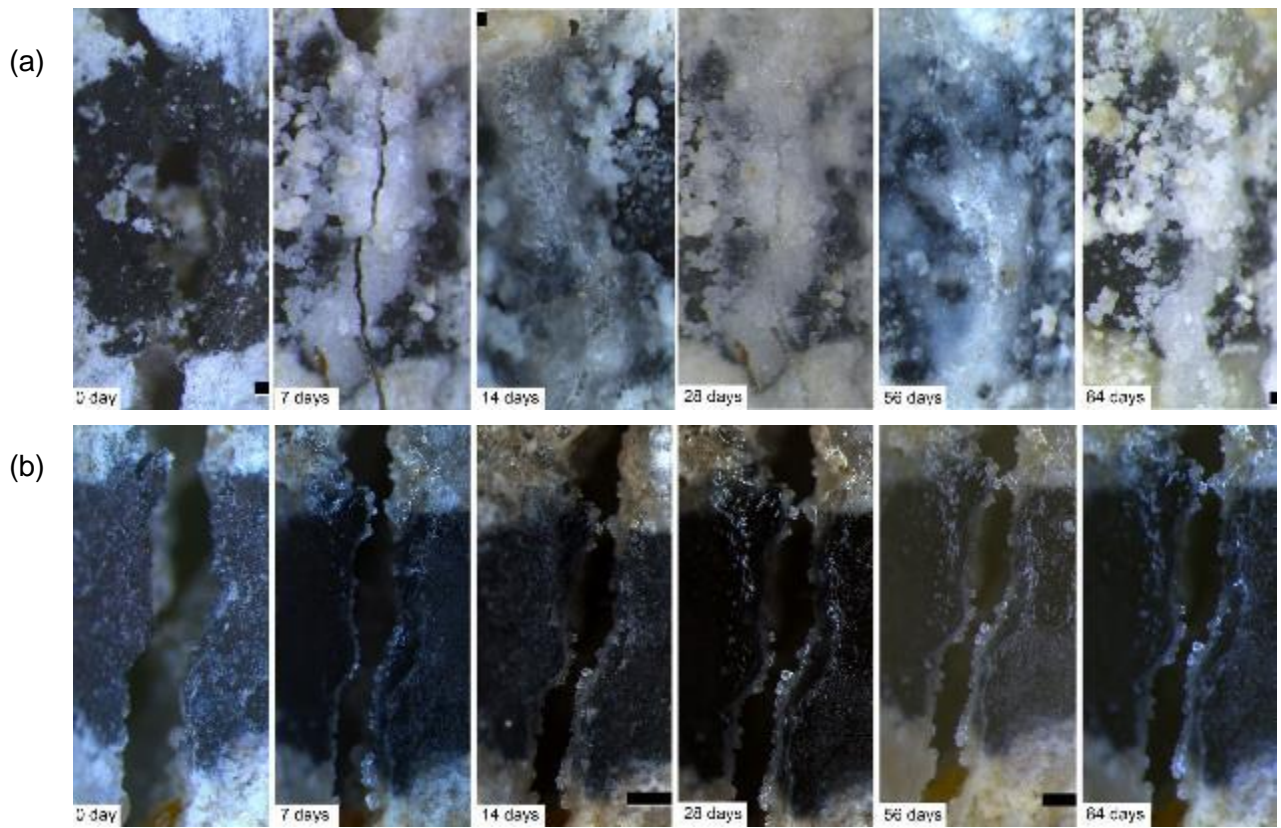


Figure S5 Progression of crack healing in (a) CaN-direct and (b) carbonated CaN-direct

732

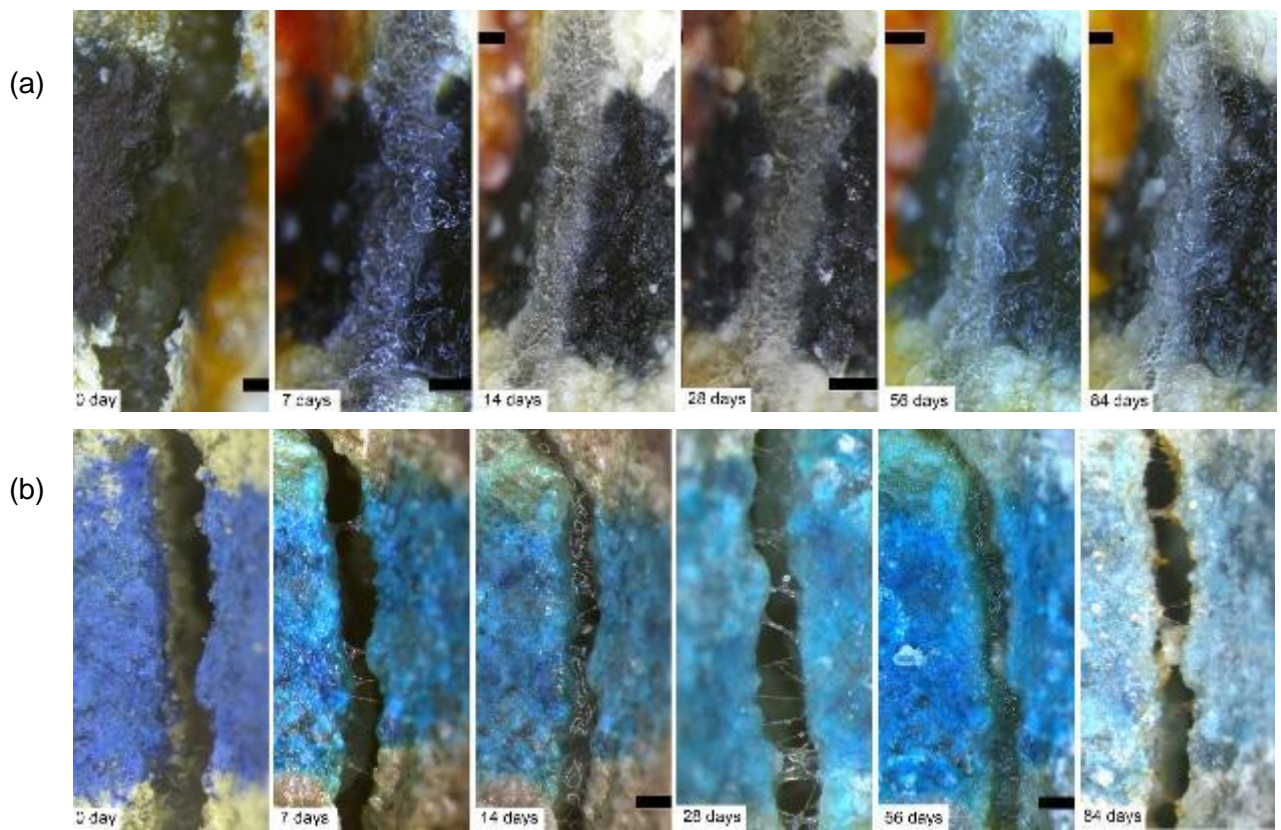


Figure S4 Progression of crack healing in (a) CaN-encap and (b) carbonated CaN-encap

733

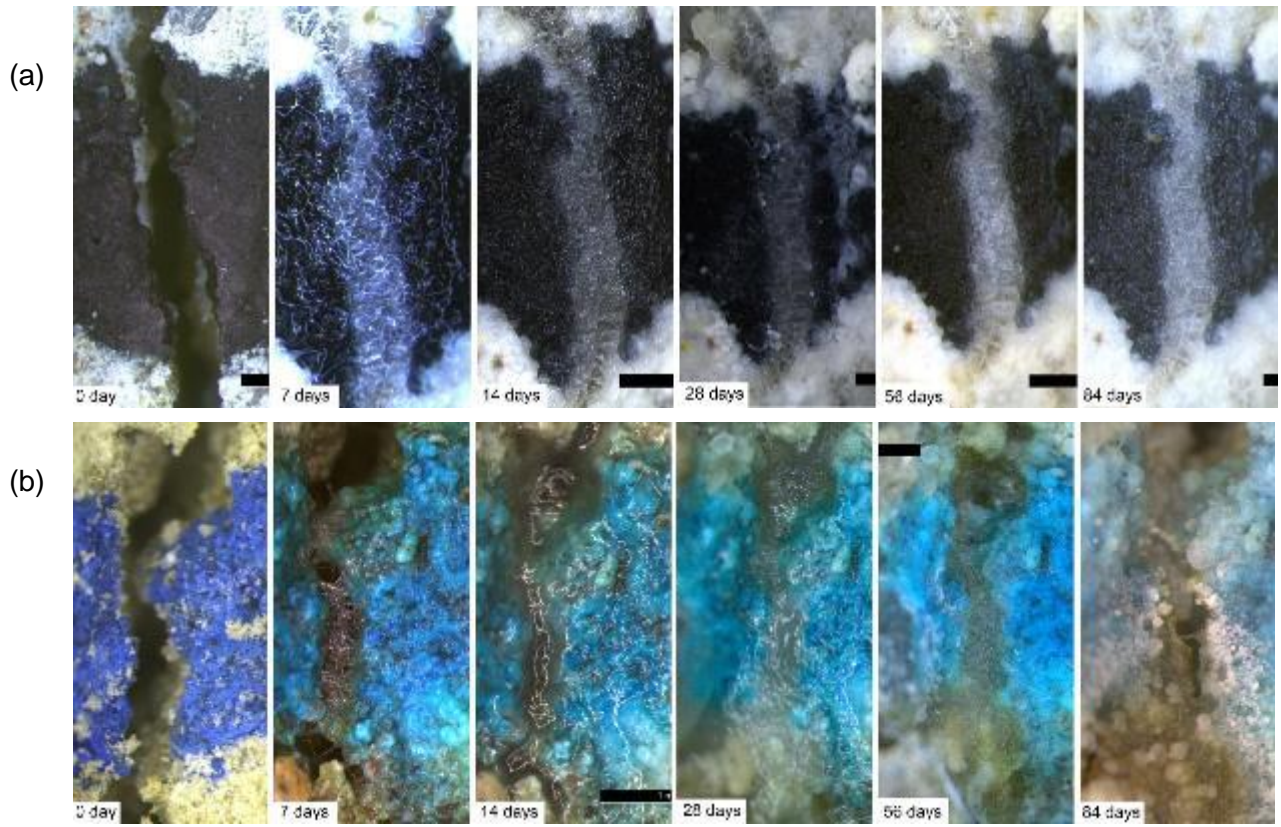


Figure S6 Progression of crack healing in (a) CaNY-encap and (b) carbonated CaNY-encap

734
735
736

737 **3. SEM and EDX images across cracks of selected mortars**

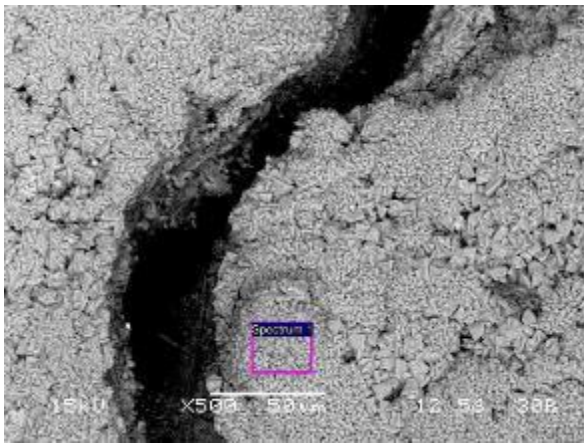
738

739 SEM images and XRD results of uncarbonated CTRL, uncarbonated CaN-direct,
740 uncarbonated CaN-encap, uncarbonated CaNY-encap and carbonated CaNY-encap are
741 shown in Figure S7-11. EDX values are included for completeness but due to the nature of
742 the techniques used the values for C and O are of limited practical application.

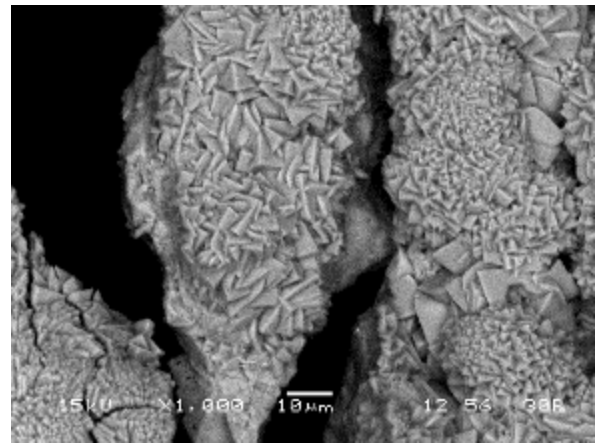
743

744

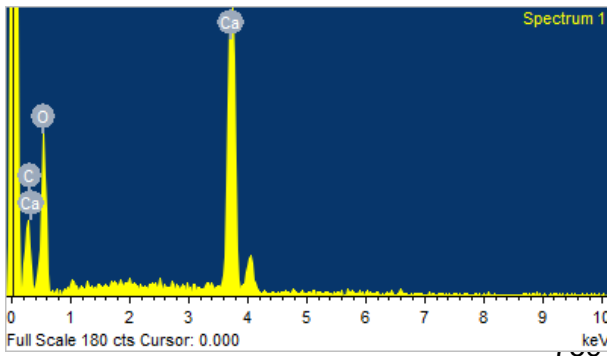
745
746
747
748
749
750
751
752
753
754
755
756



(a)



(b)



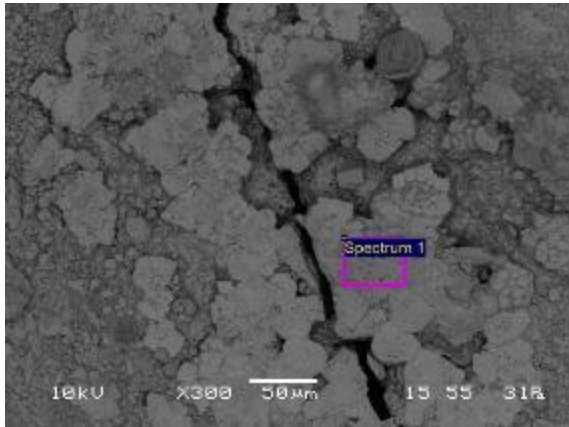
Element	Weight%	Atomic%
C K	13.26	21.42
O K	50.25	60.92
Ca K	36.49	17.66
Totals	100.00	

Figure S7 SEM and EDX of uncarbonated CTRL

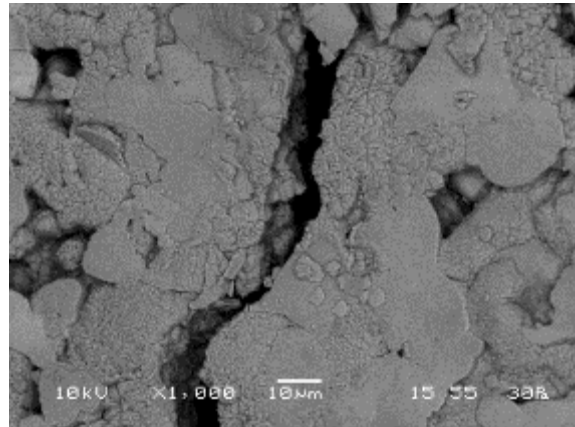
761
762

763

764



(a)

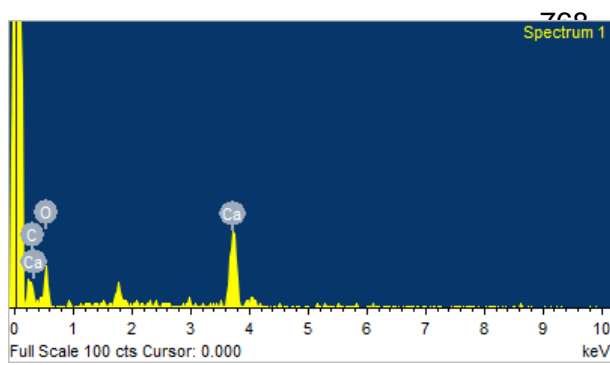


(b)

765

766

767



Element	Weight%	Atomic%
C K	10.48	18.75
O K	41.16	55.30
Ca K	48.37	25.94
Totals	100.00	

771

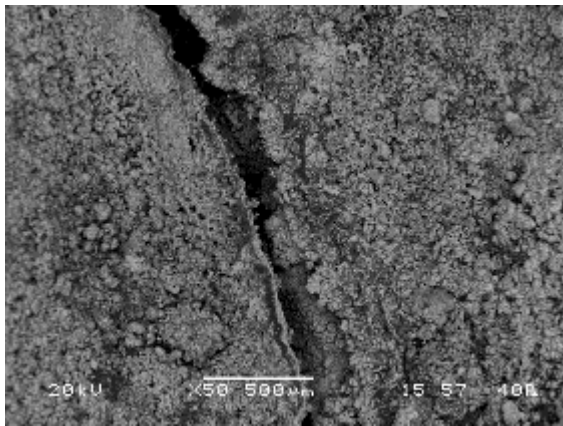
Figure S8 SEM and EDX of uncarbonated CaN-direct

72

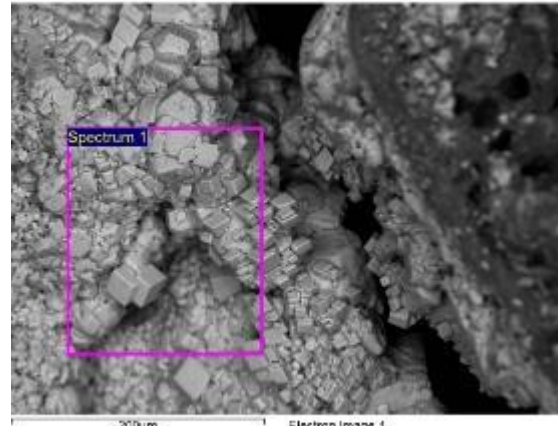
.73

774

775



(a)



(b)

776

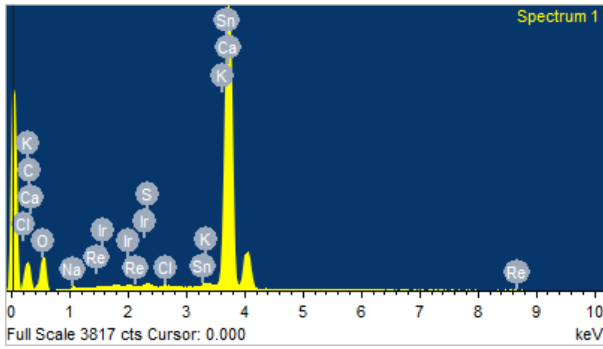


Figure S9 SEM and EDX of uncarbonated CaN-encap

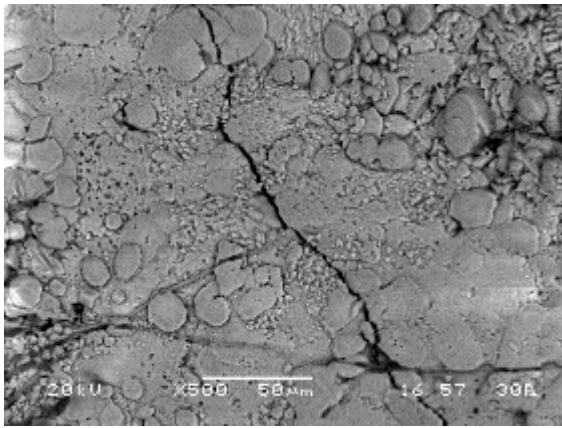
Element	Weight%	Atomic%
C K	24.78	39.35
O K	35.15	41.90
Na K	0.30	0.25
S K	0.29	0.17
Cl K	0.13	0.07
K K	0.50	0.25
Ca K	37.41	17.80
Sn L	1.10	0.18
Ir M	0.34	0.03
Totals	100.00	

777

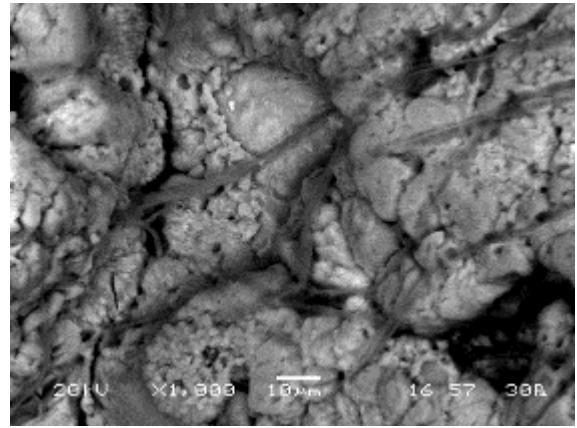
778

779

780



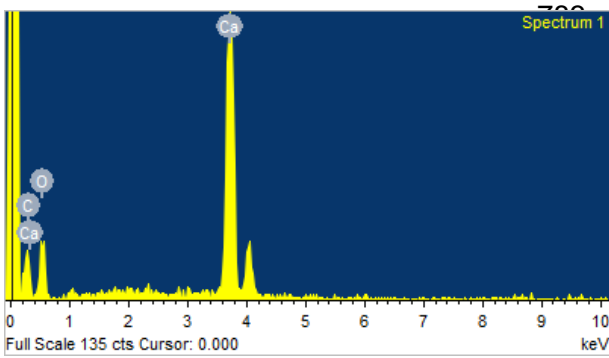
(a)



(b)

781

782



Element	Weight%	Atomic%
C K	25.74	38.70
O K	41.06	46.34
Ca K	33.20	14.96
Totals	100.00	

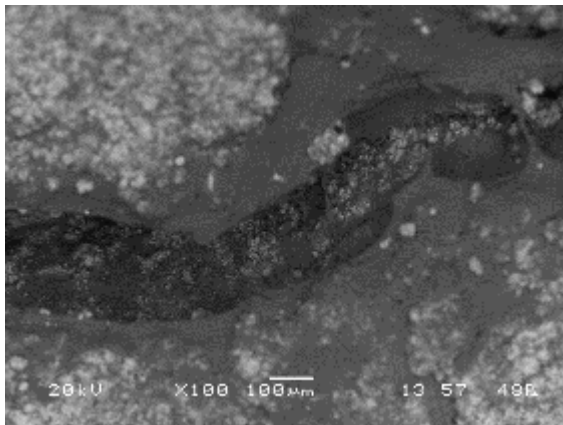
Figure S10 SEM and EDX of uncarbonated CaNY-encap

787

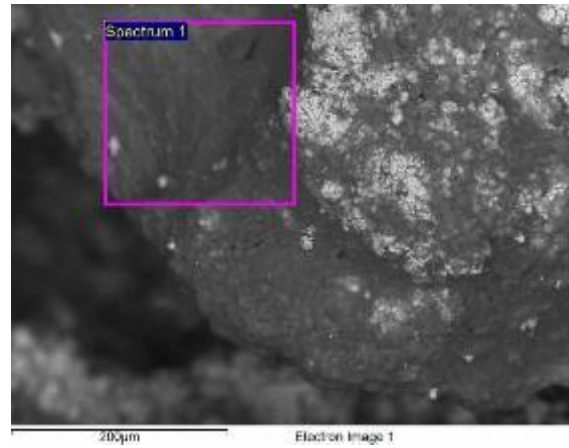
788

789

790



(a)



(b)

791

792

793

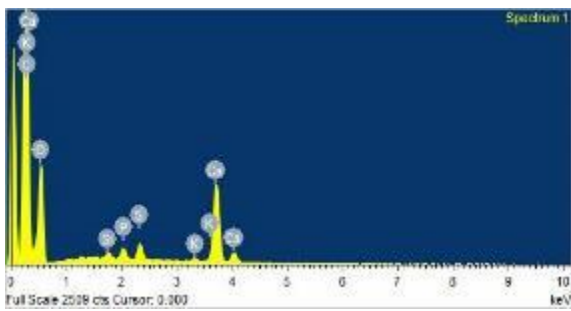


Figure S11 SEM and EDX of carbonated CaNY-encap

Element	Weight%	Atomic%
C K	60.76	69.29
O K	33.41	28.60
Si K	0.18	0.09
P K	0.43	0.19
S K	0.65	0.28
K K	0.14	0.05
Ca K	4.43	1.51
Totals	100.00	

795

796

